

# ROTATION CURVES OF SPIRAL GALAXIES

Yoshiaki Sofue<sup>1</sup> and Vera Rubin<sup>2</sup>

<sup>1</sup>*Institute of Astronomy, University of Tokyo, Mitaka Tokyo 181-0015, Japan, and*

<sup>2</sup>*Department of Terrestrial Magnetism, Carnegie Institution of Washington, Washington, DC 20015; e-mail: sofue@ioa.s.u-tokyo.ac.jp, rubin@dtm.ciw.edu*

**Abstract** Rotation curves of spiral galaxies are the major tool for determining the distribution of mass in spiral galaxies. They provide fundamental information for understanding the dynamics, evolution, and formation of spiral galaxies. We describe various methods to derive rotation curves and review the results obtained. We discuss the basic characteristics of observed rotation curves in relation to various galaxy properties, such as Hubble type, structure, activity, and environment.

## 1. HISTORICAL INTRODUCTION

The rotation of galaxies was discovered in 1914, when Slipher (1914) detected inclined absorption lines in the nuclear spectra of M31 and the Sombrero galaxy, and Wolf (1914) detected inclined lines in the nuclear spectrum of M81. This evidence led Pease (1918) to use the Mt. Wilson 60-in to “investigate the rotation of the great nebula in Andromeda” by obtaining a minor axis long slit spectrum of M31 with an exposure of 84 h taken in August, September, and October 1916, and a major axis spectrum taken over 79 h in August, September, and October 1917. The absorption lines extended only 1.5 arcmin in radius along the major axis, less than 2% of the optical radius, but were sufficient to show the steep nuclear velocity rise. Later studies of M31’s rotation by Babcock (1939) and Mayall (1951) extended major axis rotation velocities to almost 2° from the nucleus, but exposure times were tens of hours and spectrographs had stability problems. It is interesting that both Babcock’s velocities for M31 and Humason’s unpublished velocities for NGC 3115 showed the last measured point to have a rotation velocity of over 400 km s<sup>-1</sup> (almost two times actual), but they consequently raised questions of mass distribution.

Babcock’s mass model for M31 showed the mass-to-light (M/L) ratio to increase from 18 at  $r = 18'$  to 62 at  $r = 80'$ . This caused him to suggest “that absorption plays a very important role in the outer portions of the spiral, or perhaps, that new dynamical considerations are required, which will permit a smaller relative mass in the outer parts.” He concluded “the nearly constant angular velocity of the outer parts of M31 is the opposite of the ‘planetary’ type of rotation believed to obtain in the outer parts of the Galaxy.” Babcock and Oort share credit for uncovering the dark matter problem in individual spiral galaxies.

At the dedication of the McDonald Observatory in 1939, Oort (1940) noted that "... the distribution of mass [in NGC 3115] appears to bear almost no relation to that of the light." His conclusion concerning the mass distribution in NGC 3115 is worth quoting, even 60 years later. "In the outer parts of the nebula the ratio  $f$  of mass density to light density is found to be very high; and this conclusion holds for whatever dynamical model we consider. The spectrum of the nebula shows the characteristics of G-type dwarfs. Since  $f$  cannot be much larger than 1 for such stars, they can account for roughly only 1/2 percent of the mass; the remainder must consist either of extremely faint dwarfs having an average ratio of mass to light of about 200 to 1 or else of interstellar gas and dust." Current mass models of a universe with  $\Omega = 1$  also show that luminous matter composes only 1/2 percent of the mass.

Schwarzschild (1954) reanalyzed the (scattered) velocities for M31, and fit a mass model of constant M/L, and hence reaffirmed that mass followed light. Even more sweeping was de Vaucouleurs' (1959) conclusion for each of the eight galaxies with rotation velocities; beyond the velocity maximum "the rotation velocity decreases with increasing distance from the center and tends asymptotically toward Kepler's third law." With hindsight, we now view these observations as a scatter of points. We recognize that successful efforts to discriminate among models of dark matter mass distributions require high signal-to-noise velocities, which were not available until recently. Schwarzschild's and de Vaucouleurs' studies played a role in making it possible for astronomers to ignore the strange rotation curves identified by Babcock, Oort, and Mayall.

The modern era of optical observations of rotation velocities within spiral galaxies dates from Page (1952) and especially the observations by Burbidge & Burbidge (1960), which exploited the new red sensitivity of photographic plates to observe the H $\alpha$  and [NII] emission lines arising from HII regions within spiral disks. Within a decade, rotation curves existed for a few dozen galaxies, most of them extending only over the initial velocity rise and the turnover of the velocities.

Early radio observations of neutral hydrogen in external galaxies showed a slowly falling rotation curve for M31 (van de Hulst et al. 1957) and a flat rotation curve for M33 (Volders 1959). The first published velocity field ("spider diagram") was of M31 (Argyle 1965). For M33, the flatness could be attributed to the side lobes of the beam and was consequently ignored. Volders must also have realized that a flat rotation curve conflicted with the value of the Oort constants for our Galaxy, which implied a falling rotation curve at the position of the sun. Jan Oort was one of her thesis professors. By the 1970s, flat rotation curves were routinely detected (Rogstad & Shostak 1972), but worries about side bands still persisted, and a variation in mass-to-luminosity (M/L) ratio across the disk was a possible explanation (Roberts & Rots 1973).

Surveys of galaxy observations from these early years by de Vaucouleurs (1959) and of galactic dynamics by Lindblad (1959) reveal the development of the observations and the interpretation of the spiral kinematics. They are historically notable because they contain early references, many of which have faded into

oblivion. More recent (but still early) reviews include de Vaucouleurs & Freeman (1973), Burbidge & Burbidge (1975), Roberts (1975), and van der Kruit & Allen (1978).

Rotation curves are tools for several purposes: for studying the kinematics of galaxies; for inferring the evolutionary histories and the role that interactions have played; for relating departures from the expected rotation curve form to the amount and distribution of dark matter; for observing evolution by comparing rotation curves in distant galaxies with galaxies nearby. Rotation curves derived from emission lines such as H $\alpha$ , HI, and CO lines, are particularly useful to derive the mass distribution in disk galaxies, because they manifest the motion of interstellar gas of population I, which has much smaller velocity dispersion, of the order of 5–10 km s $^{-1}$ , compared with the rotation velocities. This allows us to neglect the pressure term in the equation of motion for calculating the mass distribution to a sufficiently accurate approximation.

Here, we review the general characteristics of rotation curves for spiral galaxies as kinematic tracers, in relation to galaxy properties, such as Hubble types, activity, structure, and environment. These parameters are fundamental input for understanding the dynamics and mass distribution, evolution, and formation of spiral galaxies. Methods for analysis are described. In general, the discussion is restricted to studies since 1980. Higher-order, nonaxisymmetric velocity components due to spiral arms and bars are not emphasized here. Although rotation curves of spiral galaxies are a major tool for determining the distribution of mass in spiral galaxies, we stress the observations rather than the mass determinations or the deconvolutions into luminous and dark matter components.

Numerous discussions of rotation properties are included in Merritt et al. (1999), Combes et al. (2000), and Funes & Corsini (2001). Reviews of dark matter as deduced from galaxy rotation curves can be found in Trimble (1987), Ashman (1992), and Persic & Salucci (1997 and papers therein).

Spheroidal galaxies have been reviewed earlier (Faber & Gallagher 1979, Binney 1982, de Zeeuw & Franx 1991). Generally, measures of velocity and velocity dispersions are necessary for mass determinations in early type galaxies (Poveda 1958), although methods we describe below are applicable to the cold disks often found in the cores of ellipticals, in extended disks of low-luminosity ellipticals (Rix et al. 1999), and in S0 galaxies.

Data for several million galaxies are available from huge databases accessible on the World Wide Web. Hypercat (Lyon/Meudon Extragalactic Database, <http://www-obs.univ-lyon1.fr/hypercat/>) classifies references to spatially resolved kinematics (radio/optical/1-dimension/2-dim/velocity dispersion, and more) for 2724 of its over 1 million galaxies. NED (NASA/IPAC Extragalactic Database, <http://nedwww.ipac.caltech.edu/index.html>) contains velocities for 144,000 galaxies. The number of measured velocity points is tabulated for each galaxy reference. Both of these sites contain extensive literature references for galaxy data. High spatial (HST) STIS (space telescope imaging spectrographs) spectroscopy preprints are found in <http://www.STScI.edu/science/preprints>.

## 2. THE DATA

When Burbidge & Burbidge (1960) initiated their observational program to determine the kinematics and hence masses of spiral galaxies, they were reproducing the technique employed by Pease (1918), but with improvements. Telescopes were larger, spectrographs were faster, photographic plates were sensitive in the red. The strong emission lines of H $\alpha$  and [NII] could be more easily detected and measured than could the weak broad H and K absorption lines. Since the 1980s, larger telescopes and improved detectors have existed for optical, radio, and millimeter observations. The combination of high spatial and high spectral resolution digital detectors and speedy computers has permitted a sophistication in the velocity analyses (Section 3) that will surely continue.

### 2.1. H $\alpha$ and Optical Measurements

Optical astronomers have available several observing techniques for determining rotation curves and velocity fields for both ionized gas and stars. Traditional long slit spectra are still valuable for deducing the rotation curve of a galaxy from emission lines (Rubin et al. 1980, 1982a, 1985, Mathewson et al. 1992, Mathewson & Ford 1996, Amram et al. 1992, 1994, Corradi et al. 1991, Vega Baltran 1999), but methods that return the entire velocity field, such as Fabry-Perot spectrographs (Vaughan 1989) or integral (fiber-optic) field instruments (Krabbe et al. 1997), offer more velocity information at the price of more complex and time-consuming reductions. Although H $\alpha$ , [NII], and [SII] emission lines have traditionally been employed, the Seyfert galaxy NGC 1068 has become the first galaxy whose velocity field has been studied using the infrared [Si VI] line (Tecza et al. 2000). Distant planetary nebulae (Section 2.5) and satellite galaxies are valuable test particles for determining the mass distribution at large distances from galaxy nuclei. For a limited number of nearby galaxies, rotation curves can be produced from velocities of individual HII regions in galactic disks (Rubin & Ford, 1970, 1983, Zaritsky et al. 1989, 1990, 1994).

### 2.2. HI Line

The HI line is a powerful tool to obtain kinematics of spiral galaxies, in part because its radial extent is often greater, sometimes 3 or 4 times greater, than that of the visible disk. Bosma's thesis (1978, 1981a,b) and a review of rotation curves by van der Kruit & Allen (1978) played a fundamental role in establishing the flatness of spiral rotation curves. Instrumental improvements in the past 20 years have increased the spatial resolution of the beam, so that problems arising from low resolution are important only near the nucleus or in special cases (Section 4). Although comparison of the inner velocity rise for NGC 3198 showed good agreement between the 21-cm and the optical velocities (van Albada et al. 1985, Hunter et al. 1986), the agreement was poor for Virgo spirals observed at low HI resolution (Guhathakurta et al. 1988, Rubin et al. 1989). For low-surface-brightness

galaxies, there is still discussion over whether the slow velocity rise is an attribute of the galaxy or due to the instrumentation and reduction procedures (Swaters 1999, 2001, de Blok et al. 2001) (Section 7.5).

### 2.3. CO Line

The rotational transition lines of carbon monoxide (CO) in the millimeter wave range [e.g., 115.27 GHz for  $^{12}\text{CO}$  ( $J = 1-0$ ) line, 230.5 GHz for  $J = 2-1$ ] are valuable in studying rotation kinematics of the inner disk and central regions of spiral galaxies, for extinction in the central dusty disks is negligible at CO wavelengths (Sofue 1996, 1997). Edge-on and high-inclination galaxies are particularly useful for rotation curve analysis in order to minimize the uncertainty arising from inclination corrections, for which extinction-free measurements are crucial, especially for central rotation curves.

Because the central few kiloparsecs of the disk are dominated by molecular gas (Young & Scoville 1991, Young et al. 1995, Kenney & Young 1988, Garcia-Burillo et al. 1993, Nakai et al. 1994, Nishiyama & Nakai 1998, Sakamoto et al. 1999), the molecular fraction, the ratio of the molecular-gas mass density to that of total molecular and HI masses, usually exceeds 90% (Sofue et al. 1995, Honma et al. 1995). CO lines are emitted from molecular clouds associated with star formation regions emitting the H $\alpha$  line. Hence, CO is a good alternative to H $\alpha$ , and also to HI in the inner disk, where HI is often weak or absent. The H $\alpha$ , CO, and HI rotation curves agree well with each other in the intermediate region disks of spiral galaxies (Sofue 1996, Sofue et al. 1999a,b). Small displacements between H $\alpha$  and CO rotation curves can arise in the inner regions from the extinction of the optical lines and the contamination of the continuum star light from central bulges.

Decades ago, single-dish observations in the millimeter wave range had angular resolutions limited from several to tens of arcseconds due to the aperture diffraction limit. Recently, however, interferometric observations have achieved sub- or one-arcsecond resolution (Sargent & Welch 1993, Scoville et al. 1993, Schinnerer et al. 2000, Sofue et al. 2001), comparable to, or sometimes higher than, the current optical measurements (Figure 1). Another advantage of CO spectroscopy is its high velocity resolution of one to several kilometers per second.

### 2.4. Maser Lines

Radial velocity observations of maser lines, such as SiO, OH, and H<sub>2</sub>O lines, from circumstellar shells and gas clouds allow us to measure the kinematics of stellar components in the disk and bulge of our Galaxy (Lindqvist et al. 1992a,b, Izumiura et al. 1995, 1999, Deguchi et al. 2000). VLBI astrometry of SiO maser stars' proper motions and parallaxes as well as radial velocities will reveal more unambiguous rotation of the Galaxy in the future. VLBI measurements of water masers from nuclei of galaxies reveal circumnuclear rotation on scales of 0.1 pc around massive central black holes, as observed for NGC 4258 (Miyoshi et al. 1995) (see Section 4.4).

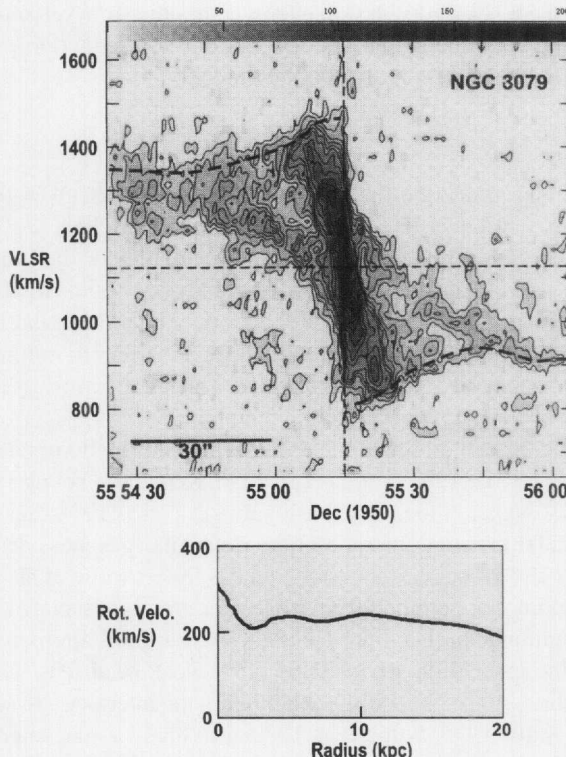


**Figure 1** Position-velocity diagram along the major axis of the edge-on galaxy NGC 3079 in the CO ( $J = 1-0$ ) line emission at a resolution of  $1.^{\prime}5$  observed with the 7-element interferometer consisting of the six-element millimeter-wave array and the 45-m telescope at Nobeyama (Sofue et al. 1999b). The lower panel shows a composite rotation curve produced by combining the CO result and HI data (Irwin & Seaquist 1991) for the outer regions.

## 2.5. Planetary Nebulae, Fabry-Perot, and Integral Field Spectrometers

Planetary nebulae are valuable tracers of the velocity fields of early type and complex galaxies, at large nuclear distances where the optical light is faint or absent (Jacoby et al. 1990, Arnaboldi et al. 1998, Gerssen 2000), and for galaxies in clusters (Cen A, Hui et al. 1995, Fornax A, Arnaboldi et al. 1998). The simultaneous analysis of absorption line velocities for inner regions and hundreds of planetary nebulae in the outer regions can constrain the viewing geometry as no single tracer can and, thus, reveal valuable details of the kinematics and the mass distribution (Rix et al. 1997, Arnaboldi et al. 1998).

Fabry-Perot spectrometers are routinely used to derive the  $H\alpha$  velocity fields of spirals of special interest (Vaughan 1989, Vogel et al. 1993, Regan & Vogel

1994, Weiner & Williams 1996). Like integral field spectrometry (Krabbe et al. 1997), these techniques will acquire more adherents as use of the instrument and reduction techniques become routine.

### 3. MEASURING ROTATION VELOCITIES

Although the mathematics of rotating disks is well established (e.g., Plummer 1911, Mestel 1963, Toomre 1982, Binney & Tremaine 1987, Binney & Merrifield 1998), the analysis of the observational data has continued to evolve as the quality of the data has improved. Both emission lines and absorption lines at a point on a spectrum are an integral along the line of sight through the galaxy. Only recently has the quality of the observational material permitted the deconvolution of various components. We describe a few procedures below.

#### 3.1. Intensity-Weighted-Velocity Method

A rotation curve of a galaxy is defined as the trace of velocities on a position-velocity (PV) diagram along the major axis, corrected for the angle between the line of sight and the galaxy disk. A widely used method is to trace intensity-weighted velocities (Warner et al. 1973). These are defined by

$$V_{\text{int}} = \int I(v)v \, dv / \int I(v) \, dv, \quad (1)$$

where  $I(v)$  is the intensity profile at a given radius as a function of the radial velocity. Rotation velocity is then given by

$$V_{\text{rot}} = (V_{\text{int}} - V_{\text{sys}}) / \sin i, \quad (2)$$

where  $i$  is the inclination angle and  $V_{\text{sys}}$  is the systemic velocity of the galaxy.

#### 3.2. Centroid-Velocity and Peak-Intensity-Velocity Methods

In outer galactic disks, where line profiles can be assumed to be symmetric around the peak-intensity value, the intensity-weighted velocity can be approximated by a centroid velocity of half-maximum values of a line profile (Rubin et al. 1980, 1982a, 1985) or, alternatively, by a velocity at which the intensity attains its maximum. This is the peak-intensity velocity (Mathewson et al. 1992, Mathewson & Ford 1996). Both methods have been adopted in deriving emission line rotation curves. Tests indicate that centroid measures of weak emission lines show less scatter (V Rubin, unpublished data).

However, for inner regions, where the line profiles are not simple but are superpositions of outer and inner-disk components, these two methods often underestimate the true rotation velocity. The same situation occurs for edge-on galaxies, where line profiles are the superposition of profiles arising from all radial distances sampled along the line of sight. In these circumstances, the envelope-tracing method described below gives more reliable rotation curves.

### 3.3. Envelope-Tracing Method (Terminal-Velocity Method)

The envelope-tracing method makes use of the terminal velocity in a PV diagram along the major axis. The rotation velocity is derived by using the terminal velocity  $V_t$ :

$$V_{\text{rot}} = (V_t - V_{\text{sys}}) / \sin i - (\sigma_{\text{obs}}^2 + \sigma_{\text{ISM}}^2)^{1/2}, \quad (3)$$

where  $\sigma_{\text{ISM}}$  and  $\sigma_{\text{obs}}$  are the velocity dispersion of the interstellar gas and the velocity resolution of observations, respectively. The interstellar velocity dispersion is of the order of  $\sigma_{\text{ISM}} \sim 7 - 10 \text{ km s}^{-1}$ , while  $\sigma_{\text{obs}}$  depends on instruments.

Here, the terminal velocity is defined by a velocity at which the intensity becomes equal to

$$I_t = [(\eta I_{\text{max}})^2 + I_{\text{lc}}^2]^{1/2} \quad (4)$$

on observed PV diagrams, where  $I_{\text{max}}$  and  $I_{\text{lc}}$  are the maximum intensity and intensity corresponding to the lowest contour level, respectively, and  $\eta$  is usually taken to be 0.2–0.5. For  $\eta = 0.2$ , this equation defines a 20% level of the intensity profile at a fixed position,  $I_t \simeq 0.2 \times I_{\text{max}}$ , if the signal-to-noise ratio is sufficiently high. If the intensity is weak, the equation gives  $I_t \simeq I_{\text{lc}}$ , which approximately defines the loci along the lowest contour level (usually  $\sim 3 \times \text{rms noise}$ ).

For nearly face-on galaxies observed at sufficiently high angular resolution, these three methods give an almost identical rotation curve. However, both finite beam width and disk thickness along the line-of-sight cause confusion of gas with smaller velocities than the terminal velocity, which often results in a lower rotation velocity in the former two methods.

The envelope-tracing method is ill-defined when applied to the innermost part of a PV diagram, for the two sides of the nucleus have a discontinuity at the nucleus due principally to the instrumental resolution. This is large with respect to the velocity gradients. In practice, this discontinuity is avoided by stopping the tracing at a radius corresponding to the telescope resolution, and then approximating the rotation curve by a straight line crossing the nucleus at zero velocity. The “solid body” rotation implied by this procedure is probably a poor approximation to the true motions near the nucleus (Section 4.3).

### 3.4. Iteration Method

An iterative method (T. Takamiya & Y. Sofue, personal communication) has been developed to derive a rotation curve. This extremely reliable method comprises the following procedure. An initial rotation curve, RC0, is adopted from a PV diagram (PV0), obtained by any method as above (e.g., a peak-intensity method). Using this rotation curve and an observed radial distribution of intensity (emissivity) of the line used in the analysis, a PV diagram, PV1, is constructed. The difference between this calculated PV diagram and the original PV0, e.g., the difference between peak-intensity velocities, is used to correct the initial rotation curve to obtain a corrected rotation curve, RC1. This RC is used to calculate another PV

diagram, PV2, using the observed intensity distribution, and to obtain the next iterated rotation curve, RC2, by correcting for the difference between PV2 and PV0. This iteration is repeated until  $PV_i$  and PV0 becomes identical, such that the summation of root mean square of the differences between  $PV_i$  and PV0 becomes minimum and stable.  $RC_i$  is adopted as the most reliable rotation curve.

### 3.5. Absorption Line Velocities

For several decades, the Fourier quotient technique (Simkin 1974, Sargent et al. 1977) or the correlation technique (Bender 1990, Franx & Illingworth 1988) were methods of choice for determining rotation velocities within early type galaxies. Both procedures assume that the stellar absorption lines formed by the integration along the line of sight through the galaxy can be fit by a Gaussian profile. However, recent instrumental improvements confirm that even disk galaxies consist of multicomponent kinematic structures, so more sophisticated methods of analysis are required to reveal velocity details of the separate stellar components.

Various methods have been devised to account for the non-Gaussian form of the line-of-sight velocity distribution. Line profiles can be expanded into a truncated Gauss-Hermite series (van der Marel & Franx 1993), which measure the asymmetric deviations ( $h_3$ ) and the symmetric deviations ( $h_4$ ) from Gaussian. Alternatively, one can use the unresolved Gaussian decomposition method (Kuijken & Merrifield 1993). Other procedures to determine line profiles and their higher order moments (e.g. Bender 1990, Rix & White 1992, Gerhard 1993) are in general agreement (Fisher 1997). Differences arise from signal-to-noise, resolution, and template mismatch. Such procedures will define the future state of the art.

### 3.6. Dependence on Observational Methods

Disk galaxies are a complex combination of various structural components. Observations from emission lines and absorption lines in the optical, millimeter, and radio regions may not sample identical regions along the same line of sight. Instruments sample at different sensitivities with different wavelength and spatial resolutions. Results are a function of the techniques of observations and reductions. A simple “rotation curve” is an approximation as a function of radius to the full velocity field of a disk galaxy. As such, it can be obtained only by neglecting small-scale velocity variations, and by averaging and smoothing rotation velocities from both sides of the galactic center. Because it is a simple, albeit approximate, description of a spiral velocity field, it is likely to be valuable even as more complex descriptions become available for many galaxies.

## 4. CENTRAL ROTATION CURVES

Centers of galaxies are still mysterious places. For galaxies as close as the Virgo cluster,  $0.1''$  subtends about 8 pc. Only in a few special cases can the stellar or gas kinematics be inferred on such scales. For very few galaxies can we sample

velocity fields on scales of tens of parsecs. Generally, when astronomers discuss circumnuclear rotation curves, they refer to velocities measured from spectra where a single resolution element encompasses a large fraction of the radius on which the velocities vary. "High accuracy" and "high resolution" mean high with respect the current state of the art.

#### 4.1. High-Resolution and Dynamic Range

A simulation reveals the effects of the finite resolution on the observed PV diagram for a galaxy with assumed gas and mass distributions (Sofue et al. 1999b). Figure 2 shows an assumed rotation curve for a galaxy containing a central compact core, bulge, disk, and massive halo, each expressed by a Plummer potential. In the observed PV diagram, however, the central steep rise and the peaks due to the core and bulge are hardly recognized. Central rotation curves derived from observed PV diagrams generally give lower limits to the rotation velocities. In fact, this conclusion holds for virtually all procedures that do not adequately account for the finite observed resolution.

CCD spectroscopy has made it possible to derive optical rotation curves of centers of galaxies because of high dynamic range and precise subtraction of bulge continuum light (Rubin & Graham 1987, Woods et al. 1990, Rubin et al. 1997, Sofue et al. 1998, 1999b, Bertola et al. 1998). However, optical spectroscopy often encounters additional difficulty arising from extinction due to dusty nuclear disks as well as confusion with absorption features from Balmer wings of A-type stars. These problems are lessened at the wavelength of CO lines because of the negligible extinction, the high molecular gas content, and the high spatial and velocity resolution. Currently, the combination of optical and CO-line spectroscopy produces rotation curves of high accuracy, reliable for the entire regions of galaxies, including the central regions (Sofue 1996, 1997, Sofue et al. 1997, 1998, 1999a,b).

In a few special cases, nuclear disks have been studied with other techniques. For several bright radio cores, HI absorption features have revealed high-velocity central disks (Ables et al. 1987, Irwin & Seaquist 1991). Rapidly rotating nuclear disks studied from their water maser emission and very-high-resolution observations are discussed in Section 4.4.

#### 4.2. The Milky Way Center

By its proximity, our Galaxy provides a unique opportunity to derive a high-resolution central rotation curve (Gilmore et al. 1990). Proper-motion studies in the near-infrared show that the velocity dispersion of stars within the central 1 pc increases toward the center, indicating the existence of a massive black hole of mass  $3 \times 10^7 M_\odot$  (Genzel et al. 1997, 2000, Ghez et al. 1998).

The rotation curve varies slightly depending on the tracer. A rotation curve formed from high-resolution CO and HI-line spectroscopy (Burton & Gordon 1978, Clemens 1985, Combes 1992) shows a very steep rise in the central hundred

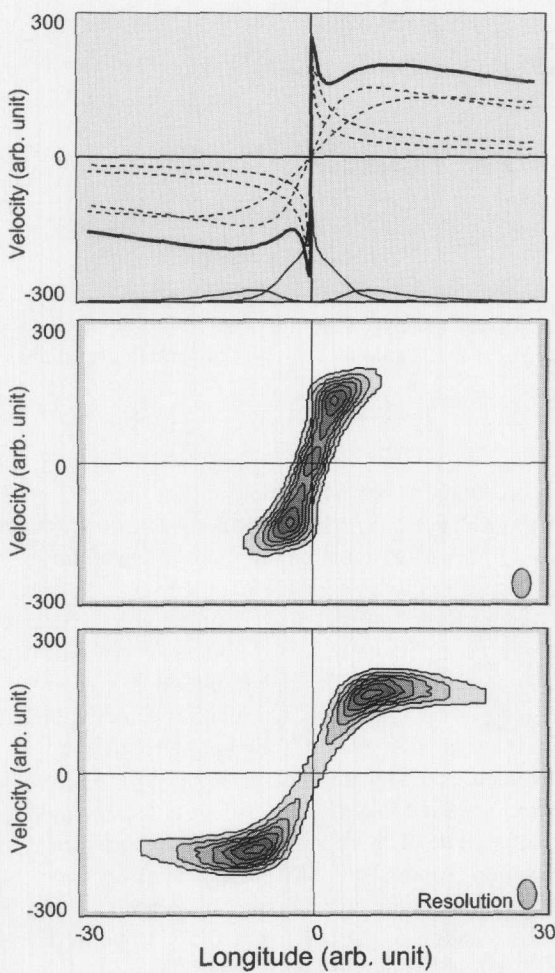


**Figure 2** Simulation of the effect of beam-smearing on a position-velocity diagram. (Top) An assumed “true” rotation curve (thick curve) comprising a central core, bulge, disk, and halo (indicated by the dashed curves, from inner to outer, respectively). Assumed density of molecular (inner) and HI gas (outer) distributions are indicated by the thin lines. (Middle) An “observed” PV diagram in CO. (Bottom) An “observed” PV diagram in HI. Both high resolution and high sensitivity are crucial to detect central high velocities and steep rise. Intensity scale is arbitrary.

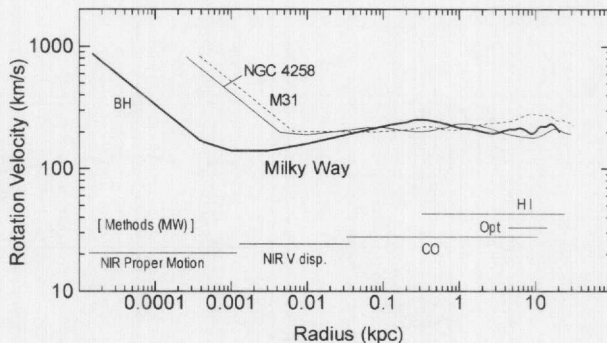


**Figure 3** Logarithmic rotation curves of the Milky Way (thick line), NGC 4258 (thin line), and M31 (dashed line). Innermost rotation velocities are Keplerian velocities calculated for massive black holes. Observational methods for the Milky Way (horizontal lines).

parsec region, attaining a peak velocity of  $250 \text{ km s}^{-1}$  at  $R \sim 300 \text{ pc}$ . HI kinematics in the bulge region indicate superposed noncircular motion, which can be attributed to a bar-driven streaming and/or expanding motion of the disk gas (Burton & Liszt 1993; see Section 4.9 for a discussion of central noncircular motions). Velocities then decrease to a minimum at  $R \sim 3 \text{ kpc}$  of about  $200 \text{ km s}^{-1}$ , followed by a gentle maximum at  $6 \text{ kpc}$  and a flat part beyond the solar circle (Blitz 1979). Rotation velocities due to the black hole are connected to the outer velocities in Figure 3. Of course, the rotation velocity does not decline to zero at the nucleus but increases inward, following a Keplerian law.

Radial velocities of OH and SiO maser lines from infrared stars in the Galactic Center region are used to derive the velocity dispersion and the mass within the observed radius. The mean rotation of the maser sources seems to take part in the Galactic rotation (Lindqvist et al. 1992a,b, Sjouwerman et al. 1998). SiO masers from IRAS sources in the central bulge have been used to study the kinematics, and the mean rotation of the bulge was found to be in solid-body rotation of the order of  $100 \text{ km s}^{-1}$  (Izumiura et al. 1995, Deguchi et al. 2000). SiO masers in the disk region have been also used to study the structure and kinematics of a possible bar structure and noncircular streaming motion superposed on the disk and bulge components (Izumiura et al. 1999).

#### 4.3. Rapidly Rotating Central Components and Massive Cores

Early observations of the core of M31 showed nuclear rapid rotation (Babcock 1939, Lallemond et al. 1960). Walker (1989) concluded from spectra taken earlier that some, but not all, galaxies exhibit rapid nuclear rotation. More recently, central rotation curves have been produced for a number of galaxies by a systematic

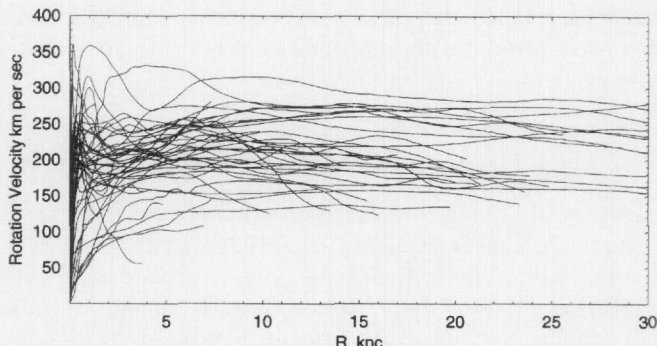


**Figure 4** Rotation curves of spiral galaxies obtained by combining CO data for the central regions, optical for disks, and HI for outer disk and halo (Sofue et al. 1999a).

compilation of PV diagrams in the CO and H $\alpha$  lines (Sofue 1996, Sofue et al. 1997, 1998, 1999a,b). Figure 4 shows rotation curves obtained for nearby galaxies at high spatial and velocity resolution. For massive spiral galaxies, high nuclear velocities may be a universal property, but they are detected only with highest resolution observations. Even a decade ago, it was observed (Rubin & Graham 1987) that innermost velocities for some galaxies start from an already high velocity at the nucleus. But high central density may not be a characteristic only of massive galaxies. The nearby galaxy M33 ( $1'' = 3$  pc), a galaxy with a minimal “bulge,” exhibits velocities over the inner  $\pm 200$  pc, which are flat at about  $V = 100 \text{ km s}^{-1}$  (Rubin 1987) and do not decrease to zero at the origin. Here, too, the contribution from the falling density of a peaked central mass exceeds the density contribution from the disk.

Bertola et al. (1998) have emphasized that the high-velocity nuclear peaks observed in some spiral galaxies match the simulated PV diagrams for Keplerian rotation due to a massive ( $\sim 10^9 M_\odot$ ) black hole, at equivalent resolution. Even more dramatic, the analysis of Maciejewski & Binney (2000) shows that when a galaxy with an arbitrarily large central velocity gradient is observed with a slit wider than the instrumental point spread function, artifacts are generated in the spectra. Such artifacts can erroneously be interpreted as discrete kinematic components and may account for some of the features observed in the spectra of Virgo galaxies (Rubin et al. 1999).

Evidence confirms that the steep nuclear rise observed in massive galaxies is real and not due to a particular view of noncircular motions. The probability of looking at a bar side-on is larger than that of viewing one end-on. Hence, there is a larger probability for apparently slower rotation than for circular velocity. For these massive galaxies, the mass density increases toward the nucleus more rapidly than expected from an exponential or de Vaucouleurs law. The widely adopted custom

of drawing a rotation curve by linking positive and negative velocities from the opposite sides across the nucleus along the major axis is incorrect, at least for these massive galaxies.

#### 4.4. Massive Black Holes and Circumnuclear Rotation

For many spirals, the innermost region exhibits rapid rotation velocities (Walker 1989, Carter & Jenkins 1993, Ford et al. 1994, van der Marel et al. 1994, Miyoshi et al. 1995, Kormendy & Richstone 1995, Richstone et al. 1998, Bertola et al. 1998, Ferrarese & Ford 1999, Kormendy & Westpfahl 1989, Kormendy 2001). These high velocities offer evidence for massive nuclear black holes. Consequently, orbital velocities in the center decrease rapidly from a velocity close to the speed of light. Detecting these high central velocities will require both enormously high spatial and velocity resolution and is a program for the future.

Currently, spectroscopic subarcsecond seeing is limited to the space telescope imaging spectrographs (STIS) and a few ground-based telescopes, except in special cases. STIS is now engaged in a major study of a sample of 54 Sb-Sc spirals,  $V \leq 2000 \text{ km s}^{-1}$  to obtain spectra at  $H\alpha$ , within a few arcseconds of the nucleus (D.J. Axon, unpublished data). The aim is to measure black hole masses, or significant upper limits.

In one very special nearby galaxy, NGC 4258, water masers at 22 GHz are observed from a disk of radius 0.1 pc in Keplerian rotation around a mass of  $3.9 \times 10^7 M_\odot$  (Nakai et al. 1993, Watson & Wallim 1994, Miyoshi et al. 1995, Herrnstein et al. 1999). The maximum rotation velocity is  $900 \text{ km s}^{-1}$ ; the rotation period is 800 years. VLBI observations of the water maser line have revealed a rapidly rotating nuclear torus of subparsec scales in several nearby active galactic nuclei (NGC 3079: Haschick et al. 1990, Trotter et al. 1998, Sawada-Satoh et al. 2000, NGC 1068: Greenhill et al. 1996, NGC 4945: Greenhill et al. 1997).

#### 4.5. Activity and Rotation Curves

One might ask whether the existence of massive objects in the nuclei, as suggested from the high central velocities, is correlated with nuclear activity. High-accuracy central rotation curves for starburst galaxies (NGC 253, NGC 1808, NGC 3034), Seyferts (NGC 1068, NGC 1097), LINERs (NGC 3521, NGC 4569, NGC 7331), and galaxies with nuclear jets (NGC 3079) (Sofue et al. 1999b, Brinks et al. 1997) show, however, no particular peculiarity. Even a very active galaxy like NGC 5128 (Cen A) shows a rotation curve much like a normal galaxy (Graham 1979). The radio lobe galaxy NGC 3079 has both strong nuclear activity and usual rotation properties, but with very high central velocities (Sofue & Irwin 1992, Irwin & Sofue 1992, Sofue et al. 1999b). While these galaxies all show a very steep central velocity rise, such steep rise is generally observed for massive galaxies without pronounced central activity. Because the global rotation and mass distribution in active spirals are generally normal, it is likely that nuclear activity is

triggered by local and temporal causes around central massive cores and/or black holes.

#### 4.6. Resonance Rings

The ring resonance in rotating disks will affect the kinematics and rotation of gas and stars in a galaxy disk. Rotation curves for several ring galaxies (Buta et al. 1995, 1999) exhibit normal rotation properties, showing a steep nuclear rise, a high-velocity peak near the resonance ring, and flat velocities in the disk and halo. Simulations of rotation properties for a bar resonance mimic well the observed variations of rotation velocities, which is of the order of  $\pm 20\text{--}30 \text{ km s}^{-1}$  (Salo et al. 1999).

#### 4.7. Nuclear Warp

A major interest in current interferometer observations of the CO line emissions from nuclear regions is the detailed orientation of the nuclear molecular disk (NMD) and circumnuclear torus. A NMD is produced by accretion of disk gas due to an angular momentum transfer to the massive disk by galactic shock waves, either in spiral arms or bars, whereas off-axis angular momentum such as associated with warping is invariant. If the accreting disk has a warp, as is often the case and is particularly prominent in mergers and interacting galaxies, the displacement of angular momentum of accreting disk from the original rotation axis is amplified. Hence, NMDs often exhibit significant warp from the main disk. Interferometric CO observations exhibit that NGC 3079's NMD is warped from the main disk by  $20^\circ$ , and contains a higher-density molecular core inclined from both the NMD and main disk (Sofue et al. 2001); NGC 1068 shows a warped nuclear disk surrounding a nuclear torus whose axis is different from that of the main disk and nuclear disk (Kaneko et al. 1997, Schinnerer et al. 2000). A nuclear warp produces uncertain inclination corrections in the rotation velocities. These can be minimized by observing edge-on galaxies.

#### 4.8. Nuclear Counterrotation

Rotating nuclear disks of cold gas have been discovered in more than 100 galaxies, types E through Sc (Bertola & Galletta 1978, Galletta 1987, 1996, Bertola et al. 1990, Bertola et al. 1992, Rubin 1994b, Garcia-Burillo et al. 1998); counterrotation is not especially rare. Simulations of disk interactions and mergers, which include gas and stellar particles (Hernquist & Barnes 1991, Barnes & Hernquist 1992), reveal that a kinematically distinct nuclear gas disk can form; it may be counterrotating. Simulation of galactic-shock accretion of nuclear gas disk in an oval potential, such as a nuclear bar, produces a highly eccentric streaming motion toward the nucleus, some portion being counterrotating (Wada & Habe 1995). Kinematically decoupled stellar nuclear disks are also observed in early type galaxies (Jedrzejewski & Schechter 1989, Franx et al. 1991). Counterrotating nuclear disks

can result from merger, mass exchange, and/or inflow of intergalactic clouds. In addition to forming the central disk, an inflow of counterrotating gas would also be likely to promote nuclear activity.

#### 4.9. Noncircular Motion in Nuclear Molecular Bar

An oval potential such is due to a bar produces galactic shocks of interstellar gas, and the shocked gas streams along the bar in noncircular orbits (Sorensen et al. 1976, Noguchi 1988, Wada & Habe 1992, 1995, Shlosman et al. 1990). The velocity of streaming motion during its out-of-shock passage is higher than the circular velocity, whereas the velocity during its shock passage is much slower than the circular velocity, close to the pattern speed of the bar in rigid-body rotation. The molecular gas is strongly concentrated in the galactic shock and stays there for a large fraction of its orbiting period. Hence, CO line velocities manifest the velocity of shocked gas. Therefore, the observed CO velocities are close to those of gas in rigid-body motion with a bar, and slower than the circular velocity. This results in underestimated rotation velocities. The viewing geometry also increases the probability that we view a bar side on, rather than end on. This too causes underestimated rotation velocities.

Bar-driven noncircular motion of the order of 20–50 km s<sup>-1</sup> is observed in central molecular disks (Ishizuki et al. 1990, Handa et al. 1990, Sakamoto et al. 1999, Kenney et al. 1992, Kohno 1998, Kohno et al. 1999). The CO-line PV diagram in the Milky Way Center (Bally et al. 1987, Oka et al. 1998, Sofue 1995) shows that the majority (~95%) of gas is rotating in steep rigid-body features. A few percent exhibit noncircular “forbidden” velocities, which could be due to noncircular motion in an oval potential (Binney et al. 1991). A question remains: Why is the majority of the gas regularly rotating? Because the gas is shocked, and intensity-weighted velocities are smaller than the circular velocity, as discussed above, determination of mass distribution in barred galaxies from observed CO velocities is not straightforward and will be a challenge for numerical simulations in the future.

### 5. DISK ROTATION CURVES

A disk rotation curve manifests the distribution of surface mass density in the disk. Simple calculation shows that the rotation velocity attains a broad maximum at a radius of about twice the scale radius for an exponential disk. For massive Sb galaxies, the rotation maximum appears at a radius of 5 or 6 kpc, which is about twice the scale length of the disk. Beyond the maximum, the rotation curve is usually flat, merging with the flat portion due to the massive dark halo. Superposed on the smooth rotation curve are fluctuations of a few tens of kilometers per second due to spiral arms or velocity ripples. For barred spirals, the fluctuations are larger, of the order of 50 km s<sup>-1</sup>, arising from noncircular motions in the oval potential.

### 5.1. Statistical Properties of Rotation Curves

The overall similarity of shapes of rotation curves for spiral galaxies has led to a variety of attempts to categorize their forms, and to establish their statistical properties. Rotation curve statistics were compiled by Roberts (1975) from HI observations, and by Burbidge & Burbidge (1975) from optical observations. Kyazumov (1984) cataloged rotation curve parameters for 116 normal S and Ir galaxies and categorized the shapes. From the galaxies they had observed, Rubin et al. (1985) formed families of Sa, Sb, and Sc synthetic rotation curves as a function of luminosity. Casertano & van Gorkom (1991), using HI velocities, studied rotation curves as a function of luminosity.

Mathewson et al. (1992) and Mathewson & Ford (1996) used their massive set of H $\alpha$  rotation curves together with optical luminosity profiles for 2447 southern galaxies to examine the Tully-Fisher (TF) (Tully & Fisher 1977) relation. For a subset of 1100 optical and radio rotation curves, Persic et al. (1995, 1996) fit the curves by a simple function of total luminosity and radius, comprising both disk and halo components. Both the forms and amplitudes are functions of the luminosity, and the outer gradient of the RC is a decreasing function of luminosity. From the same data, Roscoe (1999a,b) parameterized the outer rotation curves by a single power law as a function of radius. Numerical simulations of the formation of dark matter halos have also produced a “universal rotation curve” (Navarro et al. 1996).

Universal rotation curves reveal the following characteristics. Most luminous galaxies show a slightly declining rotation curve in the outer part, following a broad maximum in the disk. Intermediate galaxies have nearly flat rotation across the disk. Less luminous galaxies have monotonically increasing rotation velocities across the optical disk. While Persic et al. (1996) conclude that the dark-to-luminous mass ratio increases with decreasing luminosity, mass deconvolutions are far from unique.

A study of 30 spirals in the Ursa Major cluster (Verheijen 1997) showed that one third of the galaxies (chosen to have kinematically unperturbed gas disks) have velocity curves that do not conform to the universal curve shape. Rotation curves have their individualities, but they share many common characteristics. These common properties are meaningful in some situations. In other circumstances, their use may be misleading. It is important to apply the common properties only in appropriate situations, e.g., for outer disk and halo beyond  $\sim 0.5$  optical radii, corresponding to several kiloparsecs for Sb and Sc galaxies. Inner rotation curves have greater individuality (Sofue et al. 1999b).

### 5.2. Environmental Effects in Clusters

A variety of physical mechanisms can alter the internal kinematics of spirals in clusters, just as these mechanisms have affected the morphology of galaxies in clusters (Dressler 1984, Cayatte et al. 1990). Gas stripping, star stripping, galaxy-galaxy

encounters, and interaction with the general tidal field are all likely to occur. Early studies of optical rotation curves for galaxies in clusters (Burstein et al. 1986, Rubin et al. 1988, Whitmore et al. 1988, 1989) detected a correlation between outer rotation–velocity gradients and distances of galaxies from the cluster center. For distances 0.25–5 Mpc from cluster centers, inner-cluster galaxies show shallower rotation curves than do outer-cluster galaxies. These authors suggest that the outer galaxy mass is truncated in the inner-cluster environment. Later studies have failed to confirm this result (Amram et al. 1992, 1993, 1996, Sperandio et al. 1995).

A study of rotation curves for 81 galaxies in Virgo (Rubin et al. 1999, Rubin & Haltiwanger 2001) shows that about half (43) have rotation curves identified as disturbed. Abnormalities include asymmetrical rotation velocities on the two sides of the major axis, falling outer-rotation curves, inner-velocity peculiarities—including velocities hovering near zero at small radii and dips in mid-disk-rotation velocities. For these galaxies, kinematic disturbance is not correlated with morphology, luminosity, Hubble type, inclination, maximum velocity, magnitude, or local galaxy density. In contrast, the field spirals studied earlier by Rubin et al. (1985) were chosen to be isolated and without obvious morphological peculiarities. For the field galaxies, 74% exhibited rotation curves that are normal. For the Virgo sample, we attribute the rotation-curve peculiarities to the Virgo cluster environment.

Virgo spirals with disturbed kinematics have a Gaussian distribution of systemic velocities that matches that of the cluster ellipticals; spirals with regular rotation show a flat distribution. Both ellipticals and kinematically disturbed spirals are apparently in the process of establishing an equilibrium population.  $\mathrm{H}\alpha$  emission extends farther out in the disk of the disturbed spirals; the gravitational interactions have also enhanced star formation. The distribution on the sky and in systemic velocity suggests that kinematically disturbed galaxies are on elongated orbits, which carry them into the cluster core, where galaxy-cluster and galaxy-galaxy interactions are more common and stronger. Self-consistent N-body models that explore the first pass of two gravitationally interacting disk galaxies (Barton et al. 1999) produce rotation curves with midregion velocity dips matching those observed. Models of disk galaxies falling for the first time into the cluster mean field (Valluri 1993, 1994) show  $m = 1$  (warp) and  $m = 2$  (bar and spiral arms) perturbations.

### 5.3. Lopsided Position-Velocity Diagrams

As rotation curve accuracy increases, there is increased interest in galaxies with kinematically lopsided HI profiles (Baldwin et al. 1980, Sancisi 2001). These can arise from a large-scale asymmetry of HI gas distribution in the spiral disk. Of 1700 HI profiles, at least 50% show asymmetries (Richter & Sancisi 1994); recent work (Haynes et al. 1998) confirms this fraction. Because HI profiles result from an integration of the velocity and the HI distribution, resolved HI velocity fields offer more direct information on kinematic lopsidedness. From resolved HI

velocity fields, Swaters et al. (1999) also estimate the disturbed fraction to be at least 50%.

As noted above, about 50% of Virgo spirals show optical major axis velocity disturbances; how this figure translates into lopsided HI profiles is unclear. This high fraction of kinematically disturbed galaxies contrasts with the 74% of field spirals with normal kinematics. A third sample of optical rotation curves for galaxies in the Hickson groups (Rubin et al. 1991) shows noticeably lopsided rotation curves for  $\geq 50\%$ . Further studies are needed to establish the frequency of lopsidedness as a function of cluster membership, luminosity, morphology, HI content, resolution, sensitivity, and extent of the observations.

#### 5.4. Counterrotating Disks and Other Kinematic Curiosities

Only a handful of galaxies are known to have counterrotating components over a large fraction of their disks (Rubin 1994b). The disk of E7/S0 NGC 4550 (Rubin et al. 1992, Kenney & Faundez 2000) contains two cospatial stellar populations, one orbiting prograde, one retrograde. This discovery prompted modification of computer programs that fit only a single Gaussian to integrated absorption lines in galaxy spectra (Rix et al. 1992). In NGC 7217 (Sab), 30% of the disk stars orbit retrograde (Merrifield & Kuijken 1994). The bulge in NGC 7331 (Sbc) may (Prada et al. 1996), or may not, (Mediavilla et al. 1998) counterrotate with respect to the disk. Stars in NGC 4826 (Sab; the Black Eye or Sleeping Beauty) orbit with a single sense (Rubin et al. 1994). Gas extending from the nucleus through the broad dusty lane rotates prograde but reverses its sense of rotation immediately beyond; radial infall motions are present where the galaxy velocities reverse (Rubin et al. 1965, Braun et al. 1994, Rubin 1994a, Walterbos et al. 1994, Rix et al. 1995, Sil'chenko 1996).

However, galaxies with extended counterrotating disks are not common. A peculiar case is the early type spiral NGC 3593, which exhibits two cold counterrotating disks (Bertola et al. 1996). Of 28 S0 galaxies examined by Kuijken et al. (1996), none has counterrotating components accounting for more than 5% of the disk light (see also Kannappan & Fabricant 2001). Formation mechanisms for counterrotating disks can be devised (Thakar & Ryden 1998), although cases of failure are reported only anecdotally (D. Spergel, personal communication). Although such galaxies are generally assumed to be remnants of mergers, models show that generally the disk will heat up and/or be destroyed in a merger.

In an effort to circumvent the problem of disk destruction in a merger, Evans & Collett (1994) devised a mechanism for producing equal numbers of prograde and retrograde stellar disk orbits, by scattering stars off a bar in a galaxy whose potential slowly changes from triaxial to more axisymmetric. An even more dramatic solution Tremaine & Yu (2000; see also Heisler et al. 1982, van Albada et al. 1982) suggest polar rings and/or counterrotating stellar disks can arise in a disk galaxy with a triaxial halo. As the pattern speed of the initially retrograde halo changes to prograde because of infalling dark matter, orbits of disk stars caught at

the Binney resonance can evolve from prograde to retrograde disk orbits. If, instead, the halo rotation decays only to zero, stars with small inclinations are levitated (Sridhar & Touma 1996) into polar orbits. This model predicts that stellar orbits in a polar ring will be divided equally into two counterrotating streams, making this a perfect observing program for a very large telescope.

As spectral observations obtain higher resolution and sensitivity, emission from weaker components is measured. VLA observations of NGC 2403 (Fraternali et al. 2000) reveal a normal rotation, plus more slowly rotating HI extensions, the “beard.” HI detected in the forbidden velocity quadrants can be due to an infall of gas from an extended HI halo with slower rotation, perhaps from a galactic fountain flow (Schaap et al. 2000). Improved instrumentation permits detection of weaker features, so we glimpse the kinematic complexities that exist in minor populations of a single galaxy.

Edge-on and face-on spirals are fine laboratories for studying vertical kinematics. In the edge-on NGC 891, HI extends about 5 kpc above the plane, where it rotates at about  $25 \text{ km s}^{-1}$ , more slowly than the disk (Swaters et al. 1997). Slower rotation is also observed in the CO halo in the edge-on dwarf M82 (Sofue et al. 1992). Face-on galaxies such as M101 and NGC 628 often have extended HI disks showing different kinematical properties from the disks (Kamphuis et al. 1991, Kamphuis & Brigg 1992).

## 5.5. Rotation of High Redshift Galaxies

Only recently have rotation curves been obtained for distant galaxies, using HST and large-aperture ground-based telescopes with subarcsecond seeing. We directly observe galaxy evolution by studying galaxies closer to their era of formation. For galaxies whose diameters subtend only a few seconds of arc, rotation velocities for moderately distant spirals,  $z \approx 0.2\text{--}0.4$  (Bershady 1997, Bershady et al. 1999, Simard & Pritchett 1998, Kelson et al. 2000a), have already been surpassed with Keck spectra of galaxies with  $z \approx 1$  (Vogt et al. 1993, 1996, 1997, Koo 1999).

The rotation properties are similar to those of nearby galaxies, with peak velocities between 100 and 200  $\text{km s}^{-1}$ , and with flat outer-disk velocities. Regularly rotating spiral disks existed at  $z \approx 1$ , when the universe was less than half its current age. The Keck rotation velocities define a TF relation (i.e., the correlation of rotation velocity with blue magnitude) that matches to within  $\leq 0.5$  magnitudes that for nearby spirals. Therefore, spiral galaxy evolution, over the last half of the age of the universe, has not dramatically altered the TF correlation.

## 5.6. Rotation Velocity as a Fundamental Parameter of Galaxy Dynamics and Evolution

The maximum rotation velocity, reached at a few galactic-disk scale radii for average- and larger-sized spiral galaxies, is equivalent to one half the velocity width of an integrated 21-cm velocity profile. The TF relation (Tully & Fisher 1977, Aaronson et al. 1980, Aaronson & Mould 1986), which is the correlation between

total velocity width and spiral absolute magnitude, represents an oblique projection of the fundamental plane of spiral galaxies. This plane defines a three-dimensional relationship between the radius, rotation velocity, and luminosity (absolute magnitude) (Steinmetz & Navarro 1999, Koda et al. 2000a,b). The shape of a disk-rotation curve manifests the mass distribution in the exponential disk. This is perhaps the result of a dissipative process of viscous accreting gas through the proto-galactic disk evolution (Lin & Pringle 1987).

As such, the TF relation emphasizes the essential role that rotation curves play in determining the principal galactic structures, and in our understanding of the formation of disk galaxies (e.g., Mo et al. 1998). For elliptical galaxies, the three-parameter (half-light radius, surface brightness, and central velocity dispersion) fundamental plane relationship (Sandage & Perelmutter 1990a,b, Bender et al. 1992, Burstein et al. 1997) is a tool for studying elliptical galaxy evolution, analogous to the spiral TF relation. Keck spectra and HST images of 53 galaxies in cluster CL1358 + 62 ( $z = 0.33$ ) define a fundamental plane similar to that of nearby ellipticals (Kelson et al. 2000b). Ellipticals at  $z = 0.33$  are still structurally mature; data for more distant ellipticals should be available within several years.

## 6. HALO ROTATION CURVES AND DARK MATTER: A BRIEF MENTION

The difference between the matter distribution implied by the luminosity and the distribution of mass implied by the rotation velocities offers strong evidence that spiral galaxies are embedded in extended halos of dark matter. The physics of dark matter has been, and will continue to be, one of the major issues to be studied by astronomers and elementary particle physicists.

### 6.1. Flat Rotation Curve in the Halo

When Rubin & Ford (1970) published the rotation curve of M31, formed from velocities of 67 HII regions, they noted that the mass continued to rise out to the last-measured region, 24 kpc. They concluded that “extrapolation beyond that distance is clearly a matter of taste.” By 1978, Rubin et al. (1978) had learned that “rotation curves of high luminosity spiral galaxies are flat, at nuclear distances as great as 50 kpc” ( $H_0 = 50 \text{ km s}^{-1} \text{ Mpc}^{-1}$ ). Flat HI rotation curves were first noticed (Roberts & Rots 1973) using a single-dish telescope. However, it would be a few years before the observers and the theorists (Ostriker & Peebles 1973, Ostriker et al. 1974, Einasto et al. 1974) recognized each others’ work and collectively asserted that disk galaxies are immersed in extended dark matter halos. The impressive review article of Faber & Gallagher (1979) played a fundamental role in convincing the community of the need for dark matter halos around spiral galaxies.

Deeper and higher-resolution HI observations with synthesis telescopes reveal that for the majority of spiral galaxies, rotation curves remain flat beyond the

optical disks (Bosma 1981a,b, Guhathakurta et al. 1988, van Albada et al. 1985, Begeman 1989). The Sc galaxy UGC 2885 has the largest known HI disk, with HI radius of 120 kpc for  $H_0 = 50 \text{ km s}^{-1} \text{ Mpc}^{-1}$  (85 kpc for  $H_0 = 70 \text{ km s}^{-1} \text{ Mpc}^{-1}$ ); the HI rotation curve is still flat (Roelfsema & Allen 1985).

The conclusion that a flat rotation curve is due to a massive dark halo surrounding a spiral disk requires that Newtonian gravitational theory holds over cosmological distances. Although proof of this assumption is lacking, most astronomers and physicists prefer this explanation to the alternative, that Newtonian dynamics need modification for use over great distances. For readers interested in such alternatives, see Milgrom (1983), Sanders (1996), McGaugh & de Blok (1998), de Blok & McGaugh (1998), Begeman et al. (1991), and Sanders & Verheijen (1998). Nongravitational acceleration of halo gas rotation, such as is due to magneto-hydrodynamical force (Nelson 1988), is also an alternative.

## 6.2. Massive Dark Halo

One of the best indicators of dark matter is the difference between the galaxy mass predicted by the luminosity and the mass predicted by the velocities. This difference, which also produces a radial variation of the mass-to-luminosity ratio (M/L), is a clue to the distribution of visible and dark (invisible) mass (e.g., Freeman 1970, Bosma 1981a,b, Lequeux 1983, Kent 1986, 1987, Persic & Salucci 1988, 1990a,b, Salucci & Frenk 1989, Salucci et al. 1991, Forbes 1992, Persic et al. 1996, Héraudeau & Simien 1997, Takamiya & Sofue 2000). Unfortunately, there is not yet a model-independent procedure for determining the fraction of mass contained in the bulge, disk, and dark halo, and mass deconvolutions are rarely unique. Most current investigations assume that the visible galaxy consists of a bulge and a disk, each of constant M/L. Kent (1986, 1991, 1992) has used the "maximum-disk method" to derive averaged M/Ls in the individual components. Athanassoula et al. (1987) attempted to minimize the uncertainty between maximum and minimal disks by introducing constraints to allow for the existence of spiral structure. Even for our Galaxy, discussions of maximum or nonmaximum disk persist (van der Kruit 2001).

Radial profiles of the surface-mass density and surface luminosity can be used to calculate M/L directly. Forbes (1992) derived the radial variation in the ratio of the total mass to total luminosity involved within a radius,  $r$ , an "integrated M/L." Takamiya & Sofue (2000) determined the surface-mass density directly from the rotation curves, which can be sandwiched by mass distributions calculated from rotation curves on both spherical and flat-disk assumptions by solving directly the formula presented by Binney & Tremaine (1987). A comparison of the surface-mass density with optical surface photometry shows that the M/L ratio is highly variable within the optical disk and bulge and increases rapidly beyond the disk, where the dark mass dominates.

Separation of halo mass from disk mass, whether dark or luminous, is an issue for more sophisticated observations and theoretical modeling. Weiner et al.

(2001a,b) have used noncircular streaming motion to separate the two components using their theory that the streaming motion in a bar potential is sensitive to the halo mass.

### 6.3. The Extent of the Milky Way Halo

Interior to the sun's orbit, the mass of the Galaxy is  $\approx 10^{11} M_{\odot}$ . Although there is some evidence that the halo rotation curve is declining beyond 17 kpc in a Keplerian fashion (Honma & Sofue 1997a), the mass distribution beyond the HI disk, e.g., at  $> 22$  kpc, is still controversial. Interior to the distance of the Large Magellanic Cloud (LMC), the Galaxy mass may grow to  $6 \times 10^{11} M_{\odot}$  (Wilkinson & Evans 1999), depending on the assumed orbit of the Cloud. Interior to 200 kpc, the mass is at least  $2 \times 10^{12} M_{\odot}$  (Peebles 1995), matching masses for a set of Milky Way-like galaxies with masses inferred statistically from the velocities of their satellite galaxies (Zaritsky 1992).

A Milky Way halo that extends at least 200 kpc is close to the half-way distance between the Galaxy and M31, 350 kpc. And if halos are as large as those suggested by the gravitational distortion of background galaxies seen in the vicinity of foreground galaxies (Hoekstra 2000, Fischer et al. 2000), then the halo of our Galaxy may brush the equivalently large halo of M31.

### 6.4. Declining Rotation Curves

Very few spirals exhibit a true Keplerian decline in their rotation velocities. Among peculiar rotation curves, declining rotation curves are occasionally observed, confirming the conventional belief that the mass distribution is truncated at about one to three optical radii (three to five scale lengths) (Casertano 1983, Casertano & van Gorkom 1991, Barteldrees & Dettman 1994). Yet some galaxies exhibit Keplerian rotation curves well beyond the critical truncation radius (Honma & Sofue 1997a,b). Although truncation is an important issue for those who wish to weaken the notion of a conspiracy of luminous and dark matter (Casertano & van Gorkom 1991), the issue is far from resolved.

## 7. GALAXY TYPES AND ROTATION CHARACTERISTICS

For galaxies with different morphologies, ranging from Sa to Sc, there is a marked similarity both in form (though not amplitude) and in disk and halo rotation curves (Rubin et al. 1985). Thus, the form of the gravitational potential in the disk and halo is not strongly dependent on the form of the optical luminosity distribution. Some moderate correlation is found between total luminosity and rotation velocity amplitude. Also, less luminous galaxies tend to show increasing outer-rotation curve, whereas most massive galaxies have slightly declining rotation in the outmost part (Persic et al. 1996). On the other hand, the form of central rotation curve depends on the total mass and galaxy type (Sofue et al. 1999a,b). Massive galaxies of the

Sa and Sb types show steeper rises and higher central velocities within a few hundred parsecs of the nucleus compared with less-massive Sc galaxies and dwarfs. Dwarf galaxies generally show gentle central rises.

### 7.1. Sa, Sb, and Sc Galaxies

The maximum rotation velocities for Sa galaxies are higher than those of Sb and Sc galaxies with equivalent optical luminosities. Median values of  $V_{\max}$  decrease from 300 to 220 to 175 km s<sup>-1</sup> for the Sa, Sb, and Sc types, respectively (Roberts 1978, Rubin et al. 1985, Sandage 2000).

Sb galaxies have rotation curves with slightly lower values of the maximum velocity than do Sa galaxies (Rubin et al. 1985). The steep central rise at 100–200 pc is often associated with a velocity peak at radii  $r \sim 100$ –300 pc (Sofue et al. 1999b). The rotation velocity then declines to a minimum at  $r \sim 1$  kpc and is followed by a gradual rise to a broad maximum, arising from the disk potential. The disk rotation curve has superposed amplitude fluctuations of tens of kilometers per second caused mainly by spiral arms. The outermost parts are usually flat because of the massive dark halo. Some Sb galaxies show a slight outer decline, often no larger than the inner undulations (Honma & Sofue 1997a,b).

The rotation curve of the Milky Way Galaxy, a typical Sb galaxy, is shown in Figure 3 (Clemens 1985, Blitz 1979, Brand & Blitz 1993, Fich et al. 1989, Merrifield 1992, Honma & Sofue 1995, 1996). The rotation curve of Sb galaxies, including the Milky Way, can be described as having (a) a high-density core, including the massive black hole, which causes a nonzero velocity very close to the center; (b) a steep rise within the central 100 pc; (c) a maximum at radius of a few hundred parsecs, followed by a decline to a minimum at 1–2 kpc; (d) a gradual rise to maximum at 6 kpc due to the main disk; and (e) a nearly flat outer-rotation curve.

Sc galaxies have lower maximum velocities than do Sa and Sb galaxies (Roberts 1978, Rubin et al. 1980, 1985, Sandage 2000), ranging from  $\leq 100$  to  $\sim 200$  km s<sup>-1</sup>. Massive Sc galaxies show steep nuclear rises similar to those of Sb galaxies. However, less-massive Sc galaxies have more gentle rises. They also have flat rotation to their outer edges. Low-surface-brightness Sc galaxies have gentle central rises with monotonically increasing rotation velocities toward the edge, similar to dwarf galaxies (Bosma et al. 1988).

### 7.2. Barred Galaxies

Large-scale rotation properties of SBb and SBc galaxies are generally similar to those of nonbarred galaxies of Sb and Sc types. However, the study of their kinematics is more complicated than for nonbarred spirals because their gas tracers are less uniformly distributed (Bosma 1981a, 1996) and their iso-velocity contours are skewed in the direction toward the bar (H $\alpha$ , Peterson et al. 1978, HI, Sancisi et al. 1979, stellar absorption lines, Kormendy 1983). CO-line mapping and spectroscopy reveal high concentration of molecular gas in shocked lanes along a

bar superposed on significant noncircular motions (Handa et al. 1990, Sakamoto et al. 1999).

Thus, barred galaxies show velocity jumps from  $\pm\sim 30\text{--}40 \text{ km s}^{-1}$  to  $\geq 100 \text{ km s}^{-1}$  on the leading edges of the bar,  $R \sim 2\text{--}5 \text{ kpc}$ . Nonbarred spirals can show velocity variation of about  $\pm 10\text{--}20 \text{ km s}^{-1}$ , caused mainly by spiral arms. Compared with nonbarred spirals, barred galaxies require a more complete velocity field to understand their kinematics. As discussed earlier, intensity-weighted velocities are underestimated compared with the circular velocities, which is particularly crucial for shock-compressed molecular gas in the central regions (see Section 4.9).

This large velocity variation arises from the barred potential of several kiloparsec length. Simulations of PV diagrams for edge-on barred galaxies show many fluctuations of tens of kilometers per second, superposed on the usual flat rotation curve (Athanassoula & Bureau 1999, Bureau & Athanassoula 1999, Weiner & Sellwood 1999). However, distinguishing the existence of a bar and quantifying it are not uniquely done from such limited edge-on information. For more quantitative results, two-dimensional velocity analyses are necessary (Wozniak & Pfenniger 1997). In these models, barred spirals contain up to 30% counterrotating stars; the orbits are almost circular and perpendicular to the bar. Pattern speeds for the bar have been determined from absorption line spectra (Buta et al. 1996, Gerssen 2000 and references therein).

Because of their kinematic complexity, barred galaxies have been observed considerably less than have nonbarred galaxies, even though they constitute a considerable fraction of all disk galaxies (Mulchaey & Regan 1997). However, high-resolution optical observations, combined with HI and CO, have helped to stimulate the study of two-dimensional noncircular velocity fields (e.g. Wozniak & Pfenniger 1997, Hunter & Gottesman 1996, Buta et al. 1996). Gas-streaming motions along the bar are an efficient way to transport gas to the nuclear regions (Sorensen et al. 1976, Noguchi 1988, Wada & Habe 1992, 1995, Wada et al. 1998, Shlosman et al. 1990), and lead to enhanced star formation.

### 7.3. Low-Surface-Brightness Galaxies; Dwarf Galaxies

Until the past decade, observations of rotational kinematics were restricted to spirals with average or high surface brightness. Only within the past decade have low-surface-brightness galaxies been found in great numbers (Schombert & Bothun 1988, Schombert et al. 1992); many are spirals. Their kinematics were first studied by de Blok et al. (1996) with HI, who found slowly rising curves that often continued rising to their last measured point. However, many of the galaxies are small in angular extent, so observations are subject to beam smearing. Recent optical rotation curves (Swaters 1999, 2001, Swaters et al. 2000, de Blok et al. 2001) reveal a steeper rise for some, but not all, of the LSBs that previously had only 21-cm observations. It is not now clear whether low-surface-brightness galaxies are as dominated by dark matter as they were previously thought to be; the mass models have considerable uncertainties.

Dwarf galaxies, galaxies of low mass, are often grouped with low-surface-brightness galaxies, either by design or by error. The two classes overlap in the low-surface-brightness/low-mass region. However, some low-surface-brightness galaxies are large and massive; some dwarf galaxies have high surface brightness. Early observations showed dwarf galaxies to be slowly rotating, with rotation curves that rise monotonically to the last measured point (Tully et al. 1978, Carignan & Freeman 1985, Carignan & Puche 1990a,b, Carignan & Beaulieu 1989, Puche et al. 1990, 1991a,b, Lake et al. 1990, Sandage & Hoffman 1991, Broeils 1992, Sandage & Fomalont 1993). The dark matter domination of the mass of the dwarf galaxy NGC 3109 (Carignan 1985, Jobin & Carignan 1990) is confirmed by a reanalysis, including H $\alpha$  Fabry-Perot data (Blais-Ouellette et al. 1999, S. Blais-Ouellette, P. Amram & C. Carignan, submitted for publication). An exceptional case of a declining outer-rotation curve has been found in the dwarf galaxy NGC 7793 (Carignan & Puche 1990a). H $\alpha$  velocity field observations of blue compact galaxies, with velocities of less than 100 km s $^{-1}$ , show that rotation curves rise monotonically to the edges of the galaxies (Östlin et al. 1999).

Swaters (1999) derived rotation curves from velocity fields obtained with the Westerbork synthesis radio telescope for 60 late-type dwarf galaxies of low luminosity. By an interactive analysis, he obtained rotation curves that are corrected for a large part of the beam smearing. Most of the rotation curve shapes are similar to those of more luminous spirals; at the lowest luminosities, there is more variation in shape. Dwarfs with higher central light concentrations have more steeply rising rotation curves, and a similar dependence is found for disk rotation curves of spirals (Figure 5). For dwarf galaxies dominated by dark matter, as for low-surface-brightness (and also high-surface-brightness) spirals, the contributions of the stellar and dark matter components to the total mass cannot be unambiguously derived. More high-quality observations and less-ambiguous mass deconvolutions, perhaps including more physics, will be required to settle questions concerning the dark matter fraction as a function of mass and/or luminosity.

#### 7.4. The Large Magellanic Cloud

The LMC is a dwarf galaxy showing irregular optical morphology, with the enormous starforming region, 30 Dor, located significantly displaced from the optical bar and HI disk center. High-resolution HI kinematics of the LMC (Kim et al. 1998; for a review, see Westerlund 1999) indicate, however, a regular rotation around the kinematical center, which is displaced 1.2 kpc from the center of the optical bar as well as from the center of star-forming activity (Figure 6). The rotation curve has a steep central rise, followed by a flat rotation with a gradual rise toward the edge. This implies that the LMC has an invisible compact bulge, an exponential disk, and a massive halo. This dynamical bulge is 1.2 kpc away from the center of the stellar bar and is not associated with an optical counterpart. The “dark bulge” has a large fraction of dark matter, with an anomalously high mass-to-luminosity (M/L) ratio (Sofue 1999). In contrast, the stellar bar has a smaller M/L ratio compared with that of the surrounding regions.

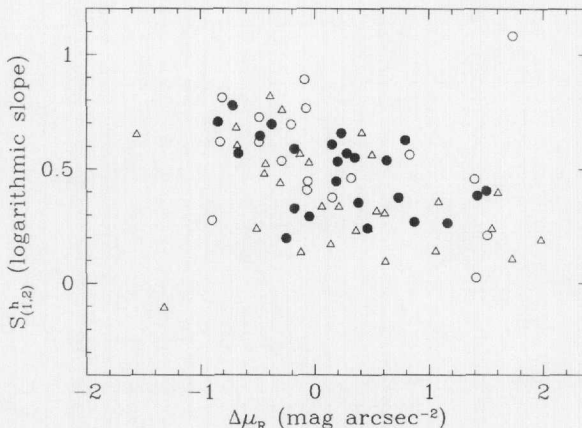


**Figure 5** The logarithmic rotation curve slope,  $S_{(1,2)}^h$  between one and two scale lengths, plotted against the central concentration of light,  $\Delta\mu_R = \mu_{0,\text{exp}} - \mu_{c,\text{obs}}$ , where  $\mu_{0,\text{exp}}$  is the extrapolated surface brightness of the exponential disk and  $\mu_{c,\text{obs}}$  is the observed central brightness (in magnitude). For pure disk systems,  $\Delta\mu_R = 0$ . Filled circles: dwarfs (high accuracy); open circles: dwarfs (low accuracy); triangles: spirals. [Courtesy of R. Swaters (1999).]

## 7.5. Irregular Galaxies: Interacting and Merging

Rotation curves for irregular galaxies are varied. Some irregular galaxies exhibit normal rotation curves, such as observed for a ring galaxy NGC 660, amorphous galaxy NGC 4631, and NGC 4945 (Sofue et al. 1999b).

The interacting galaxy NGC 5194 (M51) shows a peculiar rotation curve, which declines more rapidly than Keplerian at  $R \sim 8\text{--}12$  kpc. This may be due to inclination varying with the radius, e.g., warping. Because the galaxy is viewed nearly face-on ( $i = 20^\circ$ ), a slight warp causes a large error in deriving the rotation velocity. If the galaxy's outer disk at 12 kpc has an inclination as small as  $i \sim 10^\circ$ , such an apparently steep velocity decrease would be observed even for a flat rotation.

When galaxies gravitationally interact, they tidally distort each other and produce the pathological specimens that had until recently defied classification. In an innovative paper, Toomre (1977; see also Toomre & Toomre 1972, Holmberg 1941) arranged 11 known distorted galaxies “in rough order of completeness of the imagined mergers” starting with the Antennae (NGC 4038/39) and ending with NGC 7252. Observers rapidly took up this challenge, and Schweizer (1982) suggested that NGC 7252 is a late-stage merger, in which the central gas disks of the two original spirals still have separate identities.

There is now an extensive literature both observational and computational (Schweizer 1998 and references therein; Barnes & Hernquist 1992, 1996, Hibbard et al. 2000) that makes it possible to put limits on the initial masses, the

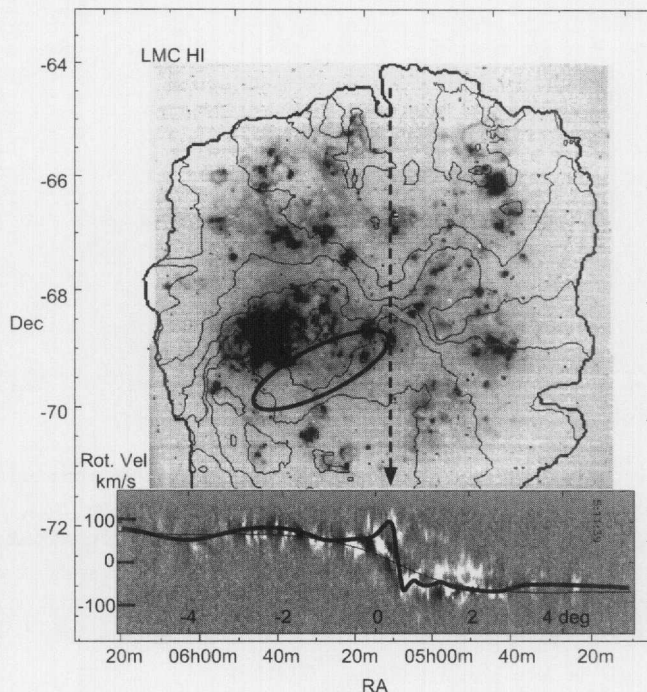


**Figure 6** The HI velocity field of the large Magellanic cloud (LMC) superposed on an H $\alpha$  image, and a position-velocity diagram across the kinematical major axis. [Courtesy of S. Kim (Kim et al. 1998).] (Ellipse) Indicates the position of the optical bar; (thick line) in PV diagram, traces the rotation curve, corrected for the inclination angle of 33°.

gas quantities, the time since the initial encounter, and the evolutionary history of the merger remnant. Equally remarkable, tidal tails can be used as probes of dark matter halos (Dubinski et al. 1999).

Many nearby galaxies appear to be products of mergers and, hence, have been extensively studied. NGC 5128 (Cen A) has a long history of velocity observations, with few signs of being completely untangled yet (H $\alpha$  long slit, Graham 1979, H $\alpha$  Fabry-Perot, Bland-Hawthorn et al. 1997, CO, Phillips et al. 1987, HI, van Gorkom et al. 1990, planetary nebulae, Hui et al. 1995).

The starburst dwarf galaxy NGC 3034 (M82) shows an exceptionally peculiar rotation (Burbidge et al. 1964, Sofue et al. 1992). It has a normal steep nuclear rise and rotation velocities that have a Keplerian decline beyond the nuclear peak. This may arise from a tidal truncation of the disk and/or halo by an encounter with M81 (Sofue 1998).

Some of the past and present history of the Milky Way and the Local Group is written in the warp of the Milky Way (I. Garcia-Ruiz, K. Kuijken & J. Dubinski, submitted for publication), in the tidal disruption of the Sagittarius dwarf (Ibata

et al. 1995), in the mean retrograde motion of the younger globular clusters (Zinn 1993), in the tidal streams in the halo (Lynden-Bell & Lynden-Bell 1995), and in the orbits of the Magellanic clouds and the Magellanic stream (Murai & Fujimoto 1980, Gardiner & Naguchi 1996; for an excellent discussion, see Schweizer 1998).

## 7.6. Polar Ring Galaxies

Polar ring galaxies provide a unique opportunity to probe the rotation and mass distribution perpendicular to galaxy disks and, hence, the three-dimensional distribution of the dark matter (Schweizer et al. 1983, Combes & Arnabaldi 1996, Sackett & Sparke 1990, Sackett et al. 1994, van Driel et al. 1995). The conclusion of Schweizer et al. (1983) from emission line velocities, that the halo mass is more nearly circular than flattened, has been contested by Sackett & Sparke (1990) based on both emission and absorption line data. However, the data are limited and velocity uncertainties are large, so the conclusions are not robust.

A major surprise comes from the study of the polar ring galaxy NGC 4650A. Arnabaldi et al. (1997; see also van Gorkom et al. 1987) discovered an extended HI disk coplanar with the ring, which twists from almost edge-on to more face-on at large radii. The K-band optical features and the HI velocities can be fit simultaneously with a model in which spiral arms are present in this polar disk. Hence the polar ring is a very massive disk. This result strengthens previous suggestions that polar ring galaxies are related to spirals (Arnabaldi et al. 1995, Combes & Arnabaldi 1996).

## 8. THE FUTURE

Most of what we know about rotation curves we have learned in the past 50 years, due principally to instrumental and computational advances. It is likely that these advances will accelerate in the future. We can look forward to an exciting future. Specifically, we can expect the following.

1. Extinction-free rotation kinematics in the central regions will come from high- $J$  CO line spectroscopy and imaging using ALMA, the Atacama Large Millimeter- and Submillimeter-wave Array at 5000-m altitude. This array will produce high spatial (0.01 arcsec) and high velocity ( $\delta V < 1 \text{ km s}^{-1}$ ) resolution.
2. Extinction-free measurements will also come from 8- and 10-m class telescopes using Br $\gamma$ , H<sub>2</sub> molecular, and other infrared lines in K-band and longer-wavelength spectroscopy.
3. VLBI spectroscopic imaging of maser sources will teach us more about super massive black holes and rotation and mass distribution in nuclear disks.
4. Rotation of the Galaxy, separately for the disk and bulge, will be directly measured from proper motions, parallaxes, and, hence, distances and radial velocities of maser sources using microarcsecond radio interferometry. The

VERA project (VLBI Experiment for Radio Astrometry) will become a prototype. This facility will also derive an independent measurement of the Galactic Center distance,  $R_0$ .

5. Optical interferometry may permit us to "watch" a nearby spiral (M31, M33, LMC) rotate on the plane of the sky, at least through a few microarcseconds. Radio interferometry of maser stars will be used to directly measure rotation on the sky of the nearest galaxies, from measures of proper motion (hence distances) and radial velocities.
6. Rotation curves will be determined for galaxies at extremely high redshift; we may be able to observe protogalactic rotation and dynamical evolution of primeval galaxies. This may be a task for successive generations of space telescopes.
7. We may be able to ultimately understand details of barred spiral velocity fields from spectroscopic imaging. We may also be able to separate the disk, bulge, and bar potentials by fitting the number of parameters necessary for describing a bar's mass and dynamical properties.
8. Polar-ring kinematics will be understood, especially halo kinematics perpendicular to the disk and, therefore, three-dimensional halo structures. We are certain to learn of details about galaxies that are unexpected and hence surprising.
9. Sophisticated methods of analysis, perhaps involving line shapes and velocity dispersions, will produce more accurate rotation curves for large samples of spirals. These will lead to more tightly constrained mass deconvolutions. Distribution of dark and luminous matters within the halo, disk, bulge, and core will be mapped in detail from more sophisticated M/L ratio analyses.
10. Dark halos may finally be understood. We will know their extent and their relation to the intracluster dark mass. We may even know the rotation velocity of the halo. Will the concept of a "rotation curve" apply at such large distances from the disk? Will we learn if our halo brushes the halo of M31?
11. We will ultimately know what is the dark matter—the major mass constituent of the Universe. Elementary particle physics will teach us its origin and physical properties.
12. Perhaps we will be able to put to rest the last doubt about the applicability of Newtonian gravitational theory on a cosmic scale, or enthusiastically embrace its successor.

#### ACKNOWLEDGMENTS

We thank Dr. Yoichi Takeda for assisting in gathering and selecting the references from a huge number of related papers over the decades. We thank Drs. Linda Dressel, Jeffrey Kenney, Stacy McGaugh, and Rob Swaters for references and helpful comments. We also thank Mareki Honma for references and Jin Koda and

Kotaro Kohno for NMA data analyses. We are indebted to Dr. Allan Sandage, the editor, for careful reading of the manuscript and for invaluable comments.

Visit the Annual Reviews home page at [www.AnnualReviews.org](http://www.AnnualReviews.org)

## LITERATURE CITED

- Aaronson M, Mould J, Huchra J. 1980. *Ap. J.* 237:655
- Aaronson M, Mould J. 1986. *Ap. J.* 303:1
- Ables JG, Forster JR, Manchester RN, Rayner PT, Whiteoak JB, et al. 1987. *Mon. Not. R. Astron. Soc.* 226:157
- Amram P, Balkowski C, Boulesteix J, Cayatte V, Marcelin M, Sullivan WT III. 1996. *Astron. Astrophys.* 310:737
- Amram P, Le Coarer E, Marcelin M, Balkowski C, Sullivan WT III, Cayatte V. 1992. *Astron. Astrophys. Suppl.* 94:175
- Amram P, Marcelin M, Balkowski C, Cayatte V, Sullivan WT III, Le Coarer E. 1994. *Astron. Astrophys. Suppl.* 103:5
- Amram P, Sullivan WT III, Balkowski C, Marcelin M, Cayatte V. 1993. *Ap. J. Lett.* 403:L59
- Argyle E. 1965. *Ap. J.* 141:750
- Arnaboldi M, Freeman KC, Gerhard O, Matthias M, Kudritzki RP, et al. 1998. *Ap. J.* 507:759
- Arnaboldi M, Freeman KC, Sackett PD, Sparke LS, Capaccioli M. 1995. *Planet. Space Sci.* 43:1377
- Arnaboldi M, Oosterloo T, Combes F, Freeman KC, Koribalski B. 1997. *Astron. J.* 113:585
- Ashman KM. 1992. *PASP* 104:1109
- Athanassoula E, Bosma A, Papaioannou S. 1987. *Astron. Astrophys.* 179:23
- Athanassoula E, Bureau E. 1999. *Ap. J.* 522:699
- Babcock HW. 1939. *Lick Obs. Bull.* 19:41
- Baldwin JE, Lynden-Bell D, Sancisi R. 1980. *Mon. Not. R. Astron. Soc.* 193:313
- Bally J, Stark AA, Wilson RW, Henkel C. 1987. *Ap. J. Suppl.* 65:13
- Barnes JE, Hernquist L. 1992. *Annu. Rev. Astron. Astrophys.* 30:705
- Barnes JE, Hernquist L. 1996. *Ap. J.* 471:115
- Barteldrees A, Dettmar R-J. 1994. *Astron. Astrophys. Suppl.* 103:475
- Barton EJ, Bromley BC, Geller MJ. 1999. *Ap. J. Lett.* 511:L25
- Begeman KG. 1989. *Astron. Astrophys.* 223:47
- Begeman KG, Broeils AH, Sanders RH. 1991. *Mon. Not. R. Astron. Soc.* 249:523
- Bender R. 1990. *Astron. Astrophys.* 229:441
- Bender R, Burstein D, Faber SM. 1992. *Ap. J.* 411:153
- Bershady MA. 1997. See Persic & Salucci 1997. 117:537
- Bershady MA, Haynes MP, Giovanelli R, Andersen DR. 1999. See Merritt et al. 1999. 182:499
- Bertola F, Bettoni D, Buson LM, Zeillinger WW. 1990. In *Dynamics and Interactions of Galaxies*, ed. ER Weilen, p. 249. Springer: Heidelberg
- Bertola F, Buson LM, Zeillinger WW. 1992. *Ap. J. Lett.* 401:L79
- Bertola F, Cappellari M, Funes JG, Corsini EM, Pizzella A, Vega Bertran JC. 1998. *Ap. J. Lett.* 509:93
- Bertola F, Cinzano P, Corsini EM, Pizzella A, Persic M, Salucci P. 1996. *Ap. J. Lett.* 458:67
- Bertola F, Galletta G. 1978. *Ap. J. Lett.* 226:115
- Binney J, Gerhard OE, Stark AA, Bally J, Uchida KI. 1991. *Mon. Not. R. Astron. Soc.* 252:210
- Binney J. 1982. *Annu. Rev. Astron. Astrophys.* 20:399
- Binney J, Merrifield M. 1998. *Galactic Astronomy*. Princeton, NJ: Princeton Univ. Press
- Binney J, Tremaine S. 1987. *Galactic Dynamics*. Princeton, NJ: Princeton Univ. Press
- Blais-Ouellette S, Carignan C, Amram P, Cote S. 1999. *Astron. J.* 118:2123

- Bland-Hawthorn J, Freeman KC, Quinn PJ. 1997. *Ap. J.* 490:143
- Blitz L. 1979. *Ap. J. Lett.* 231:115
- Bosma A. 1978. *The distribution and kinematics of neutral hydrogen in spiral galaxies of various morphological types*. PhD thesis, Univ. Groningen, The Netherlands. 186 pp.
- Bosma A. 1981a. *Astron. J.* 86:1825
- Bosma A. 1981b. *Astron. J.* 86:1791
- Bosma A. 1996. See Buta et al. 1996. 91:132
- Bosma A, van der Hulst JM, Athanassoula E. 1988. *Astron. Astrophys.* 198:100
- Brand J, Blitz L. 1993. *Astron. Astrophys.* 275:67
- Braun R, Walterbos RAM, Kennicutt RC, Tacconi LJ. 1994. *Ap. J.* 420:558
- Brinks E, Skillman ED, Terlevich RJ, Terlevich E. 1997. *Astrophys. & Space Sci.* 248:23
- Broeils AH. 1992. *Astron. Astrophys.* 256:19
- Burbidge EM, Burbidge GR. 1960. *Ap. J.* 132:30
- Burbidge EM, Burbidge GR. 1975. In *Stars and Stellar Systems IX: Galaxies and the Universe*, ed. A Sandage, M Sandage, J Kristian, p. 81. Chicago: Univ. Chicago Press
- Burbidge EM, Burbidge GR, Crampin DJ, Rubin VC, Prendergast KH. 1964. *Ap. J.* 139:1058
- Bureau M, Athanassoula E. 1999. *Ap. J.* 522:686
- Burstein D, Bender R, Faber SM, Nolthenius R. 1997. *Astron. J.* 114:1365
- Burstein D, Rubin VC, Ford WK Jr, Whitmore BC. 1986. *Ap. J. Lett.* 305:11
- Burton WB, Gordon MA. 1978. *Astron. Astrophys.* 63:7
- Burton WB, Liszt HS. 1993. *Astron. Astrophys.* 274:765
- Buta R, Crocker DA, Elmegreen BG, eds. 1996. *Barred Galaxies, ASP Conf. Ser.*, Vol. 91. San Francisco: Astron. Soc. Pacific
- Buta R, Purcell GB, Cobb ML, Crocker DA, Rautiainen P, Salo H. 1999. *Astron. J.* 117:778
- Buta R, van Driel W, Braine J, Combes F, Wakamatsu K, et al. 1995. *Ap. J.* 450:593
- Carignan C. 1985. *Ap. J.* 299:59
- Carignan C, Beaulieu S. 1989. *Ap. J.* 347:760
- Carignan C, Freeman KC. 1985. *Ap. J.* 294:494
- Carignan C, Puche D. 1990a. *Astron. J.* 100:394
- Carignan C, Puche D. 1990b. *Astron. J.* 100:641
- Carter D, Jenkins CR. 1993. *Mon. Not. R. Astron. Soc.* 263:1049
- Casertano S. 1983. *Mon. Not. R. Astron. Soc.* 203:735
- Casertano S, van Gorkom JH. 1991. *Astron. J.* 101:1231
- Cayatte V, van Gorkom JM, Balkowski C, Kotanyi C. 1990. *Astron. J.* 100:604
- Clemens DP. 1985. *Ap. J.* 295:422
- Combes F. 1992. *Annu. Rev. Astron. Astrophys.* 29:195
- Combes F, Arnaboldi M. 1996. *Astron. Astrophys.* 305:763
- Combes F, Mamon GA, Charmandaris V, eds. 2000. *Dynamics of Galaxies: From the Early Universe to the Present, XVth IAP Meet. ASP Conf. Ser.*, Vol. 197. San Francisco: Astron. Soc. Pac.
- Corradi RLM, Boulesteix J, Bosma A, Capaccioli M, Amram P, Marcellin M. 1991. *Astron. Astrophys.* 244:27
- de Blok WJG, McGaugh SS, Bosma A, Rubin VC. 2001. *Ap. J. Lett.* 552:L23
- de Blok WJG, McGaugh SS. 1998. *Ap. J.* 508:132
- de Blok WJG, McGaugh SS, van der Hulst JM. 1996. *Mon. Not. R. Astron. Soc.* 283:18
- Deguchi S, Fujii T, Izumiura H, Kameya O, Nakada Y, et al. 2000. *Ap. J. Suppl.* 128:571
- de Vaucouleurs G. 1959. *Handbuch Phys. Astrophys. IV* 53:311
- de Vaucouleurs G, Freeman KC. 1973. *Vistas Astron.* 14:163
- de Zeeuw T, Franx M. 1991. *Annu. Rev. Astron. Astrophys.* 29:239
- Dressler A. 1984. *Annu. Rev. Astron. Astrophys.* 22:185
- Dubinski J, Mihos JC, Hernquist L. 1999. *Ap. J.* 526:607
- Einasto J, Saar E, Kaasik A, Chernin AD. 1974. *Nature* 252:111
- Evans NW, Collett JL. 1994. *Ap. J. Lett.* 420:L67
- Faber SM, Gallagher JS. 1979. *Annu. Rev. Astron. Astrophys.* 17:135

- Ferrarese L, Ford HC. 1999. *Ap. J.* 515:583
- Fich M, Blitz L, Stark AA. 1989. *Ap. J.* 342: 272
- Fischer P, McKay TA, Sheldon E, Connolly A, Stebbins A, et al. 2000. *Astron. J.* 120:1198
- Fisher D. 1997. *Astron. J.* 113:950
- Forbes DA. 1992. *Astron. Astrophys. Suppl.* 92:583
- Ford HC, Harms RJ, Tsvetanov ZI, Hartig GF, Dressel LL, et al. 1994. *Ap. J. Lett.* 435:L27
- Franx M, Illingworth GD. 1988. *Ap. J. Lett.* 327:L55
- Franx M, Illingworth GD, de Zeeuw T. 1991. *Ap. J.* 383:112
- Fraternali F, Oosterloo T, Sancisi R, van Moorsel G. 2000. In *Gas and Galaxy Evolution, VLA 20th Anniv. Conf.*, ed. JE Hibbard, MP Rupen, JH van Gorkom. In press
- Freeman KC. 1970. *Ap. J.* 160:811
- Funes SJ, Corsini EM, eds. 2001. *Galaxy Disks and Disk Galaxies, ASP Conf. Series Vol 230*. San Francisco: Astron. Soc. Pac. In press
- Galletta G. 1987. *Ap. J.* 318:531
- Galletta G. 1996. See Buta et al. 1996. 91:429
- Garcia-Burillo S, Guelin M, Cernicharo J. 1993. *Astron. Astrophys.* 274:123
- Garcia-Burillo S, Sempere MJ, Bettoni D. 1998. *Ap. J.* 502:235
- Gardiner LT, Noguchi M. 1996. *Mon. Not. R. Astron. Soc.* 278:191
- Genzel R, Eckart A, Ott T, Eisenhauer F. 1997. *Mon. Not. R. Astron. Soc.* 291:219
- Genzel R, Pichon C, Eckart A, Gerhard OE, Ott T. 2000. *Mon. Not. R. Astron. Soc.* 317:348
- Gerhard OE. 1993. *Mon. Not. R. Astron. Soc.* 265:213
- Gerssen J. 2000. *Stellar Kinematics in Disk Galaxies*, PhD thesis, Rijksuniversiteit, Groningen, Netherlands. 83 pp.
- Ghez A, Klein BL, Morris M, Becklin EE. 1998. *Ap. J.* 509:678
- Gilmore G, King IR, van der Kruit PC. 1990. *The Milky Way as a Galaxy*. Mill Valley, CA: Univ. Sci. Books
- Graham JA. 1979. *Ap. J.* 232:60
- Greenhill LJ, Gwinn CR, Antonucci R, Barvainis R. 1996. *Ap. J. Lett.* 472:L21
- Greenhill LJ, Moran JM, Herrnstein JR. 1997. *Ap. J. Lett.* 481:L23
- Guhathakurta P, van Gorkom JH, Kotanyi CG, Balkowski C. 1988. *Astron. J.* 96:851
- Handa T, Nakai N, Sofue Y, Hayashi M, Fujimoto M. 1990. *Publ. Astron. Soc. Jpn.* 42:1
- Haschick AD, Baan WA, Schneps MH, Reid MJ, Moran JM, Güsten R. 1990. *Ap. J.* 356:149
- Haynes MP, Hogg DE, Maddalena RJ, Roberts MS, van Zee L. 1998. *Astron. J.* 115:62
- Heisler J, Merritt D, Schwarzschild M. 1982. *Ap. J.* 258:490
- Héraudeau Ph, Simien F. 1997. *Astron. Astrophys.* 326:897
- Hernquist L, Barnes JE. 1991. *Nature* 354:210
- Herrnstein JR, Moran JM, Greenhill LJ, Diamond PJ, Inoue M, et al. 1999. *Nature* 400:539
- Hibbard JE, Vacca WD, Yun MS. 2000. *Astron. J.* 119:1130
- Hoekstra H. 2000. *A Weak Lensing Study of Massive Structures*, PhD thesis. Rijksuniversiteit, Groningen, Netherlands. 148 pp.
- Holmberg E. 1941. *Ap. J.* 94:385
- Honma M, Sofue Y. 1996. *Publ. Astron. Soc. Jpn.* 49:103
- Honma M, Sofue Y. 1997a. *Publ. Astron. Soc. Jpn.* 49:453
- Honma M, Sofue Y. 1997b. *Publ. Astron. Soc. Jpn.* 49:539
- Honma M, Sofue Y, Arimoto N. 1995. *Astron. Astrophys.* 304:1
- Hui X, Ford HC, Freeman KC, Dopita MA. 1995. *Ap. J.* 449:592
- Hunter DA, Rubin VC, Gallagher JS III. 1986. *Astron. J.* 91:1086
- Hunter JH, Gottesman ST. 1996. See Buta et al. 1996. 91:398
- Ibata RA, Gilmore G, Irwin MJ. 1995. *Mon. Not. R. Astron. Soc.* 277:781
- Irwin JA, Seaquist ER. 1991. *Ap. J.* 371:111
- Irwin JA, Sofue Y. 1992. *Ap. J. Lett.* 396:L75
- Ishizuki S, Kawabe R, Ishiguro M, Okumura SK, Morita KI, et al. 1990. *Ap. J.* 355:436
- Izumiura H, Deguchi S, Fujii T, Kameya O, Matsumoto S, et al. 1999. *Ap. J. Suppl.* 125:257

- Izumiura H, Deguchi S, Hashimoto O, Nakada Y, Onaka T, et al. 1995. *Ap. J.* 453:837
- Jacoby GH, Ciardullo R, Ford HC. 1990. *Ap. J.* 356:332
- Jedrzejewski R, Schechter P. 1989. *Astron. J.* 98:147
- Jobin M, Carignan C. 1990. *Astron. J.* 100: 648
- Kamphuis J, Briggs F. 1992. *Astron. Astrophys.* 253:335
- Kamphuis J, Sancisi R, van der Hulst T. 1991. *Astron. Astrophys.* 244:29
- Kaneko N, Aoki K, Kosugi G, Ohtani H, Yoshida M, et al. 1997. *Astron. J.* 114:94
- Kannappan SJ, Fabricant DG. 2001. *Astron. J.* 121:140
- Kelson DD, Illingworth GD, van Dokkum PG, Franx M. 2000a. *Ap. J.* 531:159
- Kelson DD, Illingworth GD, van Dokkum PG, Franx M. 2000b. *Ap. J.* 531:184
- Kenney J, Young SJ. 1988. *Astrophys. J. Suppl.* 66:261
- Kenney JPD, Faundez S. 2000. In *Stars, Gas and Dust in Galaxies: Exploring the Links*, PASP Conf. Ser. San Francisco: Astron. Soc. Pac. In press
- Kenney JDP, Wilson CD, Scoville NZ, Devereux NA, Young JS. 1992. *Ap. J. Lett.* 395:L79
- Kent SM. 1986. *Astron. J.* 91:1301
- Kent SM. 1987. *Astron. J.* 93:816
- Kent SM. 1991. *Ap. J.* 378:131
- Kent SM. 1992. *Ap. J.* 387:181
- Kim S, Stavely-Smith L, Dopita MA, Freeman KC, Sault RJ, et al. 1998. *Ap. J.* 503:674
- Koda J, Sofue Y, Wada K. 2000a. *Ap. J.* 532:214
- Koda J, Sofue Y, Wada K. 2000b. *Ap. J. Lett.* 531:L17
- Kohno K. 1998. *Molecular Gas in the Central Regions of Nearby Starburst and Seyfert Galaxies*. PhD thesis. Univ. Tokyo, Tokyo, Jpn. 187 pp.
- Kohno K, Kawabe R, Villa-Vilaro B. 1999. *Ap. J.* 511:157
- Koo DC. 1999. In *Proc. XIX Moriond Meet. Build. Galaxies: From the Primordial Universe to the Present*, ed. F Hammer, TX
- Thuan, V Cayatte, B Guiderdoni J, Tran Thanh Van. Gif-sur-Yvette, France: Frontières. p. 279
- Kormendy J. 1983. *Ap. J.* 275:529
- Kormendy J. 2001. See Funes & Corsini 2001. 230:247
- Kormendy J, Richstone D. 1995. *Annu. Rev. Astron. Astrophys.* 33:581
- Kormendy J, Westpfahl DJ. 1989. *Ap. J.* 338:752
- Krabbe A, Colina L, Thatte N, Kroker H. 1997. *Ap. J.* 476:98
- Kuijken K, Fisher D, Merrifield MR. 1996. *Mon. Not. R. Astron. Soc.* 283:543
- Kuijken K, Merrifield MR. 1993. *Mon. Not. R. Astron. Soc.* 264:712
- Kyazumov GA. 1984. *Astron. Zh.* 61:846
- Lake G, Schommer RA, van Gorkom JH. 1990. *Astron. J.* 99:547
- Lallemand A, Duchesne M, Walker MF. 1960. *PASP* 72:76
- Lequeux J. 1983. *Astron. Astrophys.* 125:394
- Lin DNC, Pringle JE. 1987. *Ap. J. Lett.* 320:L87
- Lindblad B. 1959. *Handbuch Phys. Astrophys.* IV 53:21
- Lindqvist M, Habing HJ, Winnberg A. 1992a. *Astron. Astrophys.* 259:118
- Lindqvist M, Winnberg A, Habing HJ, Matthews HE. 1992b. *Astron. Astrophys. Suppl.* 92:43
- Lynden-Bell D, Lynden-Bell RM. 1995. *Mon. Not. R. Astron. Soc.* 275:429
- Maciejewski W, Binney J. 2000. In *IAU Symp. No. 205: Galaxies and their Constituents at the Highest Angular Resolution*, ed. R Schillizzi, W Sparks, M Stiavelli, Z Tsvetanov, R van der Merel, Dordrecht: Kluwer Academic. In press
- Mathewson DS, Ford VL. 1996. *Ap. J. Suppl.* 107:97
- Mathewson DS, Ford VL, Buchhorn M. 1992. *Ap. J. Suppl.* 81:413
- Mayall NU. 1951. In *The Structure of the Galaxy*. Ann Arbor: Univ. Mich. Press, p. 19
- McGaugh SS, de Blok WJG. 1998. *Ap. J.* 499:66
- Mediavilla E, Arribas S, Garcia-Lorenzo B, Del Burgo C. 1998. *Ap. J.* 488:682

- Merrifield MR. 1992. *Astron. J.* 103:1552
- Merrifield MR, Kuijken K. 1994. *Ap. J.* 432:75
- Merritt D, Sellwood JA, Valluri M, eds. 1999. *Galaxy Dynamics. ASP Conf. Ser.* Vol. 182, San Francisco: Astron. Soc. Pac.
- Mestel L. 1963. *Mon. Not. R. Astron. Soc.* 126:553
- Milgrom M. 1983. *Ap. J.* 270:371
- Miyoshi M, Moran J, Herrnstein J, Greenhill L, Nakai N, et al. 1995. *Nature* 373:127
- Mo HJ, Mao S, White SDM. 1998. *Mon. Not. R. Astron. Soc.* 295:319
- Mulchaey JS, Regan MW. 1997. *Ap. J. Lett.* 482:L135
- Murai T, Fujimoto M. 1980. *Publ. Astron. Soc. Jpn.* 32:581
- Nakai N, Inoue M, Miyoshi M. 1993. *Nature* 361:45
- Nakai N, Kuno N, Handa T, Sofue Y. 1994. *Publ. Astron. Soc. Jpn.* 46:527
- Navarro JF, Frenk CS, White SDM. 1996. *Ap. J.* 462:563
- Nelson AH. 1988. *Mon. Not. R. Astron. Soc.* 233:115
- Nishiyama K, Nakai N. 1998. In *IAU Symp. No. 184: The Central Regions of the Galaxy and Galaxies*, ed. Y. Sofue, p. 245. Dordrecht: Kluwer Academic
- Noguchi N. 1988. *Astron. Astrophys.* 203:259
- Östlin G, Amram P, Masegosa J, Bergvall N, Boulesteix J. 1999. *Astron. Astrophys. Suppl.* 137:419
- Oka T, Hasegawa T, Sato F, Tsuboi M, Miyazaki A. 1998. *Ap. J. Suppl.* 118:455
- Oort JH. 1940. *Ap. J.* 91:273
- Ostriker JP, Peebles PJE. 1973. *Ap. J.* 186:467
- Ostriker JP, Peebles PJE, Yahil A. 1974. *Ap. J. Lett.* 193:L1
- Page T. 1952. *Ap. J.* 116:63
- Pease FG. 1918. *Proc. Natl. Acad. Sci. USA* 4:21
- Peebles PJE. 1995. *Ap. J.* 449:52
- Persic M, Salucci P. 1988. *Mon. Not. R. Astron. Soc.* 234:131
- Persic M, Salucci P. 1990a. *Mon. Not. R. Astron. Soc.* 247:349
- Persic M, Salucci P. 1990b. *Mon. Not. R. Astron. Soc.* 245:577
- Persic M, Salucci P. 1995. *Ap. J. Suppl.* 99:501
- Persic M, Salucci P, eds. 1997. *Dark and Visible Matter in the Universe. ASP Conf. Ser.* Vol. 117, San Francisco: Astron. Soc. Pacific
- Persic M, Salucci P, Stel F. 1996. *Mon. Not. R. Astron. Soc.* 281:27
- Peterson CJ, Rubin VC, Ford WK Jr, Thonnard N. 1978. *Ap. J.* 219:31
- Phillips TG, Ellison BN, Keene JB, Leighton RB, Howard RJ, et al. 1987. *Ap. J. Lett.* 322:L73
- Plummer HC. 1911. *Mon. Not. R. Astron. Soc.* 71:460
- Poveda A. 1958. *Bol. Obs. Tonantzintla y Tacubaya, No.* 17:3
- Prada F, Gutierrez CM, Peletier RF, McKeith CD. 1996. *Ap. J. Lett.* 463:L9
- Puche D, Carignan C, Bosma A. 1990. *Astron. J.* 100:1468
- Puche D, Carignan C, Wainscoat RJ. 1991a. *Astron. J.* 101:447
- Puche D, Carignan C, van Gorkom JH. 1991b. *Astron. J.* 101:456
- Regan MW, Vogel SN. 1994. *Ap. J.* 434:536
- Richstone D, Ajahar EA, Bender R, Bower G, Dressler A, Faber S, et al. 1998. *Nature* 395A:14
- Richter O-G, Sancisi R. 1994. *Astron. Astrophys.* 290:9
- Rix H-W, Carollo CM, Freeman K. 1999. *Ap. J. Lett.* 513:L25
- Rix H-W, de Zeeuw PT, Cretton N, van der Marel RP, Carollo CM. 1997. *Ap. J.* 488:702
- Rix H-W, Franx M, Fisher D, Illingworth G. 1992. *Ap. J. Lett.* 400:L5
- Rix H-W, Kennicutt RC, Braun R, Walterbos RAM. 1995. *Ap. J.* 438:155
- Rix H-W, White S. 1992. *Mon. Not. R. Astron. Soc.* 254:389
- Roberts MS, Rots AH. 1973. *Astron. Astrophys.* 26:483
- Roberts MS. 1975. In *Galaxies and the Universe*, ed. A Sandage, M Sandage, J Kristian, Chicago: Univ. Chicago Press, p. 309
- Roberts MS. 1978. *Astron. J.* 83:1026
- Roelfsema PR, Allen RJ. 1985. *Astron. Astrophys.* 146:213
- Rogstad DH, Shostak GS. 1972. *Ap. J.* 176:315

- Roscoe DF. 1999a. *Astron. Astrophys.* 343:697
- Roscoe DF. 1999b. *Astron. Astrophys.* 343:788
- Rubin VC. 1994a. *Astron. J.* 107:173
- Rubin VC. 1994b. *Astron. J.* 108:456
- Rubin VC. 1987. In *IAU Symp. No. 121: Observational Evidence of Activity in Galaxies*, ed. EYe Khachikian, KJ Fricke, J Melnick, p. 461. Dordrecht, Ger.: Reidel
- Rubin VC, Burbidge EM, Burbidge GR, Pendergast KH. 1965. *Ap. J.* 141:885
- Rubin VC, Burstein D, Ford WK Jr, Thonnard N. 1985. *Ap. J.* 289:81
- Rubin VC, Ford WK Jr. 1970. *Ap. J.* 159:379
- Rubin VC, Ford WK Jr. 1983. *Ap. J.* 271, 556
- Rubin VC, Ford WK Jr, Thonnard N. 1980. *Ap. J.* 238:471
- Rubin VC, Ford WK Jr, Thonnard N. 1982a. *Ap. J.* 261:439
- Rubin VC, Graham JA. 1987. *Ap. J. Lett.* 316:L67
- Rubin VC, Graham JA, Kenney JD. 1992. *Ap. J. Lett.* 394:L9
- Rubin VC, Hiltiwanger J. 2001. In *Galaxy Disks and Disk Galaxies*, ed. J Funes, EM Corsini, ASP Conf. Ser. 230:421
- Rubin VC, Hunter DA, Ford WK Jr. 1991. *Ap. J. Suppl.* 76:153
- Rubin VC, Kenney JD, Boss AP, Ford WK Jr. 1989. *Astron. J.* 98:1246
- Rubin VC, Kenny JDP, Young JS. 1997. *Astron. J.* 113:1250
- Rubin VC, Thonnard N, Ford WK Jr. 1978. *Ap. J. Lett.* 225:L107
- Rubin VC, Thonnard N, Ford WK Jr. 1982b. *Astron. J.* 87:477
- Rubin VC, Waterman AH, Kenney JDP. 1999. *Astron. J.* 118:236
- Rubin VC, Whitmore BC, Ford WK Jr. 1988. *Ap. J.* 333:522
- Sackett PD, Rix H-W, Jarvis BJ, Freeman KC. 1994. *Ap. J.* 436:629
- Sackett PD, Sparke LS. 1990. *Ap. J.* 361:408
- Sakamoto K, Okumura SK, Ishizuki S, Scoville NZ. 1999. *Ap. J. Suppl.* 124:403
- Salo H, Rautiainen P, Buta R, Purcell GB, Cobb ML, et al. 1999. *Astron. J.* 117:792
- Salucci P, Ashman KM, Persic M. 1991. *Ap. J.* 379:89
- Salucci P, Frenk CS. 1989. *Mon. Not. R. Astron. Soc.* 237:247
- Sancisi R. 2001. In *Galaxy Disks and Disk Galaxies*, ed. J Funes, EM Corsini, ASP Conf. Ser. 230:111
- Sancisi R, Allen RJ, Sullivan WT III. 1979. *Astron. Astrophys.* 78:217
- Sandage A. 2000 *PASP* 112:504
- Sandage A, Formalont E. 1993. *Ap. J.* 407:14
- Sandage A, Hoffman GL. 1991. *Ap. J. Lett.* 379:L45
- Sandage A, Perelmuter J-M. 1990a. *Astron. J.* 350:481
- Sandage A, Perelmuter J-M. 1990b. *Astron. J.* 861:1
- Sanders RH. 1996. *Ap. J.* 473:117
- Sanders RH, Verheijen MAW. 1998. *Ap. J.* 503:97
- Sargent AI, Welch WJ. 1993. *Annu. Rev. Astron. Astrophys.* 31:297
- Sargent WLW, Schechter PL, Boksenberg A, Shortridge K. 1977. *Ap. J.* 212:326
- Sawada-Satoh S, Inoue M, Shibata KM, Kameno S, Migenes V, et al. 2000. *Publ. Astron. Soc. Jpn.* 52:421
- Schaap WE, Sancisi R, Swaters RA. 2000. *Astron. Astrophys. Lett.* 356:49
- Schinnerer E, Eckart A, Tacconi LJ, Genzel R, Downes D. 2000. *Ap. J.* 533:850
- Schombert JM, Bothun GD. 1988. *Astron. J.* 95:1389
- Schombert JM, Bothun GD, Schneider SE, McGaugh SS. 1992. *Astron. J.* 103:1107
- Schwarzchild M. 1954. *Astron. J.* 59:273
- Schweizer F. 1982. *Ap. J.* 252:455
- Schweizer F. 1998. In *Galaxies: Interactions and Induced Star Formation*, ed. RC Kennicutt Jr, F Schweizer, JE Barnes, D Friedli, L Martinet, D Pfenniger, p. 105. Berlin: Springer-Verlag
- Schweizer F, Whitmore BC, Rubin VC. 1983. *Astron. J.* 88:909
- Scoville NZ, Thakker D, Carlstrom JE, Sargent AE. 1993. *Ap. J. Lett.* 404:L59
- Shlosman I, Begelman MC, Frank J. 1990. *Nature* 345:679
- Sil'chenko KO. 1996. *Astron. Lett.* 22:108
- Simard L, Pritchett CJ. 1998. *Ap. J.* 505:96

- Simkin SM. 1974. *Astron. Astrophys.* 31: 129
- Sjouwerman LO, van Langevelde HJ, Winnberg A, Habing HJ. 1998. *Astron. Astrophys. Suppl.* 128:35
- Slipher VM. 1914. *Lowell Obs. Bull.* 62, Vol. 11, 12
- Sofue Y. 1995. *Publ. Astron. Soc. Jpn.* 47:527
- Sofue Y. 1996. *Ap. J.* 458:120
- Sofue Y. 1997. *Publ. Astron. Soc. Jpn.* 49:17
- Sofue Y. 1998. *Publ. Astron. Soc. Jpn.* 50:227
- Sofue Y. 1999. *Publ. Astron. Soc. Jpn.* 51:445
- Sofue Y, Honma M, Arimoto N. 1995. *Astron. Astrophys.* 296:33
- Sofue Y, Irwin JA. 1992. *Publ. Astron. Soc. Jpn.* 44:353
- Sofue Y, Koda J, Kohno K, Okumura SK, Honma M, et al. 2001. *Ap. J. Lett.* 547:L115
- Sofue Y, Reuter H-P, Krause M, Wielebinski R, Nakai N. 1992. *Ap. J.* 395:126
- Sofue Y, Tomita A, Honma M, Tutui Y. 1999a. *Publ. Astron. Soc. Jpn.* 51:737
- Sofue Y, Tomita A, Honma M, Tutui Y, Takeda Y. 1998. *Publ. Astron. Soc. Jpn.* 50:427
- Sofue Y, Tutui Y, Honma M, Tomita A. 1997. *Astron. J.* 114:2428
- Sofue Y, Tutui Y, Honma M, Tomita A, Takamiya T, et al. 1999b. *Ap. J.* 523:136
- Sorensen S-A, Matsuda T, Fujimoto M. 1976. *Astrophys. Space Sci.* 43:491
- Sperandio M, Chincarini G, Rampazzo R, de Souza R. 1995. *Astron. Astrophys. Suppl.* 110:279
- Sridhar S, Touma J. 1996. *Mon. Not. R. Astron. Soc.* 279:1273
- Steinmetz M, Navarro JF. 1999. *Ap. J.* 513:555
- Swaters RA. 1999. *Dark Matter in Late-Type Dwarf Galaxies*. PhD thesis, Rijksuniversiteit, Groningen, Netherlands, 185 pp.
- Swaters RA. 2001. See Funes & Corsini. 2001. 230:545
- Swaters RA, Madore BF, Trewhella M. 2000. *Ap. J. Lett.* 531:107
- Swaters RA, Sancisi R, van der Hulst JM. 1997. *Ap. J.* 491:140
- Swaters RA, Schoenmakers RHM, Sancisi R, van Albada TS. 1999. *Mon. Not. R. Astron. Soc.* 304:330
- Takamiya T, Sofue Y. 2000. *Ap. J.* 534:670
- Tecza M, Thatte N, Maiolino R. 2000. In *IAU Symp. No. 205: Galaxies and their Constituents at the Highest Angular Resolution* In press
- Thakar AR, Ryden BS. 1998. *Ap. J.* 506:93
- Toomre A. 1977. In *The Evolution of Galaxies and Stellar Populations*, ed. BM Tinsley, RB Larson, p. 401. New Haven, CT: Yale Univ. Ob.
- Toomre A. 1982. *Ap. J.* 259:535
- Toomre A, Toomre J. 1972. *Ap. J.* 178:623
- Tremaine S, Yu Q. 2000. *Mon. Not. R. Astron. Soc.* 319:1
- Trimble V. 1987. *Annu. Rev. Astron. Astrophys.* 25:425
- Trotter AS, Greenhill LJ, Moran JM, Reid MJ, Irwin Judith A, Lo K-Y. 1998. *Ap. J.* 495:740
- Tully RB, Bottinelli L, Fisher JR, Gougenheim L, Sancisi R, van Woerden H. 1978. *Astron. Astrophys.* 63:37
- Tully RB, Fisher JR. 1977. *Astron. Astrophys.* 54:661
- Valluri M. 1993. *Ap. J.* 408:57
- Valluri M. 1994. *Ap. J.* 430:101
- van Albada TS, Bahcall JN, Begeman K, Sancisi R. 1985. *Ap. J.* 295:305
- van Albada TS, Kotanyi CG, Schwarzschild M. 1982. *Mon. Not. R. Astron. Soc.* 198:303
- van de Hulst HC, Raimond E, van Woerden H. 1957. *Bull. Astron. Inst. Neth.* 14:1
- van der Kruit PC. 2001. See Funes & Corsini 2001. 230:119
- van der Kruit PC, Allen RJ. 1978. *Annu. Rev. Astron. Astrophys.* 16:103
- van der Marel M, Franx M. 1993. *Ap. J.* 407:525
- van der Marel RP, Rix HW, Carter D, Franx M, White SDM, de Zeeuw T. 1994. *Mon. Not. R. Astron. Soc.* 268:521
- van Driel W, Combes F, Casoli F, Gerin M, Nakai N, et al. 1995. *Astron. J.* 109:942
- van Gorkom JH, Schechter PL, Kristian J. 1987. *Ap. J.* 314:457
- van Gorkom JH, van der Hulst JM, Haschick AD, Tubbs AD. 1990. *Astron. J.* 99:1781
- Vaughan JM. 1989. *The Fabry-Perot Interferometer. History, Theory, Practice and*

- Applications.* The Adam Hilger Ser. Opt. Optoelectron. Bristol, UK: Hilger
- Vega Baltran JC. 1999. *Comparative Kinematics of Gas and Stars in Disc Galaxies*, PhD thesis. Tenerife, Spain: Univ. de La Laguna, 204 pp.
- Verheijen MAW. 1997. *The Ursa Major cluster of galaxies*, PhD thesis. Rijksuniversiteit, Groningen, Netherlands. 254 pp.
- Vogel SN, Rand RJ, Gruendl RA, Teuben PJ. 1993. *ASP Conf. Ser.* 105:666
- Vogt NP, Forbes DA, Phillips AC, Gronwall C, Faber SM, et al. 1996. *Ap. J. Lett.* 465:15
- Vogt NP, Herter T, Haynes MP, Courteau S. 1993. *Ap. J. Lett.* 415:L95
- Vogt NP, Phillips AC, Faber SM, Gallego J, Gronwall C, et al. 1997. *Ap. J. Lett.* 479:121
- Volders L. 1959. *Bull. Astron. Inst. Neth.* 1:323
- Wada K, Habe A. 1992. *Mon. Not. R. Astron. Soc.* 258:82
- Wada K, Habe A. 1995. *Mon. Not. R. Astron. Soc.* 277:433
- Wada K, Sakamoto K, Minezaki T. 1998. *Ap. J.* 494:236
- Walkers MF. 1989. *ASP Conf. Ser.* 101:333
- Walterbos RAM, Braun R, Kennicutt RC Jr. 1994. *Astron. J.* 107:184
- Warner PJ, Wright MCH, Baldwin JE. 1973. *Mon. Not. R. Astron. Soc.* 163:163
- Watson WD, Wallin BK. 1994. *Ap. J.* 432:35
- Weiner BJ, Sellwood JA. 1999. *Ap. J.* 524:112
- Weiner BJ, Sellwood SA, Williams TB. 2001a. *Ap. J.* 546:931
- Weiner BJ, Williams TB. 1996. *Astron. J.* 111:1156
- Weiner BJ, Williams TB, van Gorkom JH, Sellwood SA. 2001b. *Ap. J.* 546:916
- Westerlund BE. 1999. In *IAU Symp. No. 190: New Views of the Magellanic Clouds*, ed. Y-H Chu, N Suntzeff, J Hesser, D Bohlen, p. 287. Dordrecht, Netherlands: Kluwer Academic
- Whitmore BC, Forbes DA. 1989. *Astron. Astrophys. Suppl. Ser.* 156:175
- Whitmore BC, Forbes DA, Rubin VC. 1988. *Ap. J.* 333:542
- Wilkinson MI, Evans NW. 1999. *Mon. Not. R. Astron. Soc.* 310:645
- Wolf M. 1914. *Vierteljahrsschr Astron. Ges.* 49:162
- Woods D, Madore BF, Fahlman GG. 1990. *Ap. J.* 353:90
- Wozniak H, Pfenniger D. 1997. *Astron. Astrophys.* 317:14
- Young JS, Scoville NZ. 1991. *Annu. Rev. Astron. Astrophys.* 29:581
- Young JS, Xie S, Tacconi L, Knezek P, Vicuso P, et al. 1995. *Ap. J. Suppl.* 98:219
- Zaritsky D. 1992. *Publ. Astron. Soc. Pac.* 104:831
- Zaritsky D, Elston R, Hill JM. 1989. *Astron. J.* 97:97
- Zaritsky D, Elston R, Hill JM. 1990. *Astron. J.* 99:1108
- Zaritsky D, White SDM. 1994. *Ap. J.* 435:599
- Zinn R. 1993. In *The Globular Clusters-Galaxy Connection*, *ASP Conf. Ser.*, ed. GH Smith, JP Brodie, 48:38. San Francisco: Astron. Soc. Pac.